VILNIUS UNIVERSITY

AND

CENTER FOR PHYSICAL SCIENCES AND TECHNOLOGY

SAULIUS FRANKINAS

CONTROLLING OF TEMPORAL AND SPECTRAL CHARACTERISTICS OF ULTRASHORT FIBER LASERS BY NONLINEAR EFFECTS

Summary of doctoral dissertation,

Physical Sciences, Physics (02P)

Vilnius, 2018

The dissertation was prepared at the Center for Physical Sciences and Technology (CPST) in 2013-2017. The major part of the experiments was done in company EKSPLA and in Science and Technology Park of Institute of Physics.

Scientific supervisor:
Dr. Andrejus Michailovas (Center for Physical Sciences and Technology, Physical Sciences - 02P).

Scientific advisor:
Dr. Nerijus Rusteika (Center for Physical Sciences and Technology, Physical Sciences - 02P).

The doctoral thesis will be defended during open session of Doctoral Council:

Chairman:

Prof. habil. dr. Valerijus Smilgevičius (Vilnius University, Physical Sciences, Physics-02P).

Members:

1. Prof. habil. dr. Arūnas Krotkus (Center for Physical Sciences and Technology, Physical Sciences, Physics - 02P);

2. Doc. dr. Rytis Butkus (Vilnius University, Physical Sciences, Physics - 02P);

3. Dr. Kęstutis Regelskis (Center for Physical Sciences and Technology, Physical Sciences, Physics - 02P);

4. Prof. dr. Valdas Pašiškevičius (KTH Royal Institute of Technology, Physical Sciences, Physics - 02P).

This thesis will be under open consideration on 27th of April, 2018 at 10 a.m. at the hall of CPST Institute of Physics.

Address: Savanoriu Ave. 231, LT-02300 Vilnius, Lithuania.

Summary of the doctoral thesis was distributed on 27th of March, 2018.

The doctoral thesis is available at libraries of CPST and Vilnius University and accessible by link https://www.vu.lt/naujienos/ivykiu-kalendorius

VILNIAUS UNIVERSITETAS

IR

FIZINIŲ IR TECHNOLOGIJOS MOKSLŲ CENTRAS

SAULIUS FRANKINAS

ULTRATRUMPŲJŲ IMPULSŲ SKAIDULINIŲ LAZERIŲ LAIKINIŲ IR SPEKTRINIŲ CHARAKTERISTIKŲ VALDYMAS NETIESINIAIS PROCESAIS

Daktaro disertacija,

Fiziniai mokslai, Fizika (02P)

Vilnius, 2018

Disertacija rengta 2013-2017 metais Fizinių ir technologijos mokslų centro lazerinių technologijų skyriuje. Didžioji dalis eksperimentų buvo atlikta įmonės EKSPLA ir fizikos instituto mokslo ir technologijų parko laboratorijose.

Mokslinis vadovas:

Dr. Andrejus Michailovas (Fizinių ir technologijos mokslų centras, fiziniai mokslai, fizika - 02P).

Mokslinis konsultantas:

Dr. Nerijus Rusteika (Fizinių ir technologijos mokslų centras, fiziniai mokslai, fizika - 02P).

Disertacija ginama viešame disertacijos Gynimo tarybos posėdyje:

Pirmininkas:

Prof. habil. dr. Valerijus Smilgevičius (Vilniaus universitetas, fiziniai mokslai, fizika-02P).

Nariai:

1. Prof. habil. dr. Arūnas Krotkus (Fizinių ir technologijos mokslų centras, fiziniai mokslai, fizika - 02P);

2. Doc. dr. Rytis Butkus (Vilniaus universitetas, fiziniai mokslai, fizika - 02P);

3. Dr. Kęstutis Regelskis (Fizinių ir technologijos mokslų centras, fiziniai mokslai, fizika - 02P);

4. Prof. dr. Valdas Pašiškevičius (Švedijos Karališkasis technologijų institutas, fiziniai mokslai, fizika - 02P).

Disertacija bus ginama viešame disertacijos Gynimo tarybos posėdyje 2018 m. balandžio mėn. 27 d. 10 val. FTMC Fizikos instituto salėje.

Adresas: Savanorių pr. 231, LT-02300 Vilnius, Lietuva.

Disertacijos santrauka išsiuntinėta 2018 m. kovo 27 d.

Disertaciją galima peržiūrėti Vilniaus universiteto, Fizinių ir technologijos mokslų centro bibliotekose ir VU interneto svetainėje adresu:
https://www.vu.lt/naujienos/ivykiu-kalendorius

Table of Contents

Acknowledgements

List of abbreviations

CFBG   Chirped fiber Bragg grating
SAM   Semiconductor saturable absorption mirror
TCD   Total cavity dispersion
CPA   Chirped pulse amplification
CVBG   Chirped volume Bragg grating
GVD   Group velocity dispersion
TOD   Third-order dispersion
FROG   Frequency resolved optical gating
OPCPA   Optical parametric chirped pulse amplification
PCF   Photonic crystal fiber
OPA   Optical parametric amplifier
NA   Numerical aperture
BBO   Beta barium borate, (β-BaB_2O_4)
LBO   Lithium triborate
BiBO   Bismuth triborate, (BiB_3O_6)

Introduction

The opportunity to tune spectral and temporal characteristics of the fiber laser extends the application field of fiber lasers. Nowadays, the research of controlling temporal and spectral characteristics using techniques based on parametric nonlinearities, harmonic generation and continuum generation is relevant. One of the techniques, which allows tuning the central wavelength of the system is a continuum generation by pulses of a few hundred femtoseconds and the optical parametric amplification [1]. The optical parametric amplification is commonly used to tune the wavelength of femtosecond solid state lasers [2,3]. Moreover, optical parametric amplifiers (OPA) are used for generation of ultrashort, few optical cycle pulses [4,5]. Commonly those systems operate at a low repetition rate (1–200 kHz) and the generated pulse in the tunable range with the energy higher than tens of μJ [6,2]. However, the pulse energy of only tens of nJ is sufficient for biological tissues imaging, such as two or three photon microscopy [7–9]. Therefore, a laser source with the nJ energy and the higher repetition rate could be more preferable for those applications due to the high frame rate and a better signal-noise ratio [7,8]. However, the realization of the solid state laser that operates at 1 MHz repetition rate is not straightforward – various techniques that make the system more complex and of large size are applicable [8,10]. Therefore laser sources based on fiber technology are developing intensively [11,12].

Most advantages of the fiber laser are determined by geometrical properties, however the strong light localization in the fiber core creates an efficient light interaction with material. Therefore, the power and energy scaling of ultrafast single-mode fiber amplifiers is restricted due to nonlinear pulse distortions, which are enforced by the large product of intensity and interaction length inside the fiber core. This limitation can be overcome by the sufficient pulse stretching in the time domain and the enlargement of the mode-field diameter of the fiber to reduce the nonlinear effects. Nowadays large diameter fiber amplifiers based on photonic crystal fibers are well developed [13–15]. This technology enables achieving the mJ pulse energy and a few hundreds of femtosecond pulses [16–18]. However, developing fiber systems for applications that do not require a high pulse energy, more attention is paid to the compactness and reliability of the system. Therefore, techniques for controlling spectral and temporal characteristics of pulses that can be integrated into the fiber system design are developing intensively.

The controlling of temporal and spectral pulse characteristics in fiber lasers is an important part of this study. In this work much attention has been devoted to the pulse stretching, chirped pulse amplification and to the efficient compression of amplified pulses. In this work different configurations of the pulse stretcher/compressor were also investigated. One of them, a combination of the tunable dispersion pulse stretcher based on the chirped fiber Bragg grating and the chirped volume Bragg grating pulse compressor of fixed dispersion, is presented. This combination of the pulse stretcher/compressor is very attractive from the practical point of view because it allows

us to give up a diffraction grating compressor which requires a complex alignment, has a limited long-term stability, and is relatively large. Therefore, the combining of various fiber technologies allows realizing a compact fiber laser which can be applied for the frequency conversion using the optical parametric amplification. Furthermore, in this work the frequency conversion system without the need for the high peak intensity and operating at a high repetition rate was developed. Developing this system, a continuum generation in bulk crystals by pump pulses from the fiber laser that operates at the 1 MHz repetition rate was performed. The amplification of a generated continuum in BBO and BiBO nonlinear crystals was also performed. Finally, implementation of the developed methods and techniques into a wavelength-tunable laser system that generates pulses with the duration less than 150 fs in the spectral range from 700 nm up to 2040 nm is presented.

Aim and the main tasks of the thesis

The main aim of this work was to develop a femtosecond wavelength-tunable laser system based on the optical parametric amplifier (OPA) pumped by the femtosecond fiber laser. In order to develop a fiber femtosecond laser that would be suitable for OPA, operating at the MHz repetition rate, and to optimize this OPA system, the following tasks were performed:

1. To investigate the impact of low dispersion chirped fiber Bragg gratings parameters for temporal and spectral characteristics of generated pulses.
2. To investigate various concepts of the pulse stretching/compressing that allows one to achieve high fidelity pulses at the output of the system and allows one to simplify the laser structure.
3. To investigate capabilities and limitations of the chirped pulse amplification in photonic fiber amplifiers with the core diameter of 40 μm and 55 μm achieving high energy and high-fidelity femtosecond pulses at the output of the system.
4. Using fiber lasers operating at the 1 MHz repetition rate and generating hundreds of femtosecond pulses to find out optimal conditions of the continuum generation in various bulk crystals.
5. To demonstrate and investigate amplification of the generated continuum in collinear configuration OPA using the biaxial bismuth triborate (BiB_3O_6, BiBO) crystal that belongs to the borate family.

Novelty of the work

1. In this work the controlling of temporal and spectral characteristics of mode-locked soliton fiber oscillator pulses by modifying the characteristics of the fiber Bragg grating was demonstrated experimentally. This method allowed one to realize the all-in-fiber oscillator that generates pulses with the duration shorter than 1 ps. Using a low dispersion fiber Bragg grating in the oscillator, the shortest duration of pulses (380 fs) was achieved from this design oscillator operating in the passively mode-locking regime.
2. The formation of parabolic shape pulses in the fiber amplifier by use of initial pulses with the duration of 380 fs was demonstrated experimentally and theoretically. In this work the fiber system that generates linearly chirped parabolic pulses and allows achieving transform-limited pulses with the duration of 110 fs was realized experimentally.
3. In this work a novel chirped pulse amplification system consisting of the chirped fiber Bragg grating with the matched dispersion profile as a pulse stretcher and the chirped volume Bragg grating as a pulse compressor is presented for the first time to our knowledge.
4. In this work a wavelength tuning system of the fiber laser is presented. The system is based on the continuum generation in the YAG crystal and parametrical amplification in the BiBO crystal. The system is unique so that for the efficient frequency conversion a low pump energy (1 μJ) is sufficient and seed of the parametric amplifier is a continuum radiation generated by 1 MHz repetition rate pulses. This tunable femtosecond system incorporating fiber and solid-state technologies was demonstrated for the first time to our knowledge.

Importance of the work

The constant development of fiber laser technologies makes it possible to realize the compact and robust design, maintenance-free fiber laser systems generating ultrashort pulses. Combining of fiber lasers and nonlinear wavelength tuning schemes is very important for the development of compact and wavelength tuning systems that are suitable for spectroscopy applications.

From the practical point of view this thesis is important in these respects:

1. Using chirped fiber Bragg gratings that compensate normal dispersion of the cavity, the soliton mode-locked fiber oscillators generating pulses with the duration in the range of 0.38-1.2 ps were developed. These oscillators were successfully used in fiber CPA systems and for formation of parabolic pulses in the fiber amplifier.

2. In this work it was demonstrated that parabolic pulses could be generated in the fiber amplifier using relatively long pulses (380 fs) generated from a passively mode-locked fiber oscillator. This opens up the possibilities for replacing the solid-state laser with the fiber oscillator in a such system, therefore the system becomes more practical and simple.

3. The method to compensate the third order dispersion introduced by the diffraction grating pulse compressor in the fiber CPA system was demonstrated experimentally and theoretically. This method is based on the optimization of the chirp profile of the CFBG stretcher and allows one to improve the temporal quality of compressed pulses.

4. In this work a novel fiber CPA system consisting of the tunable dispersion CFBG stretcher and the fixed dispersion CVBG as a pulse compressor is presented. This pulse stretcher/compressor design opens up new opportunities for the creation of compact and insensitive for misalignment fiber CPA systems.

5. It was experimentally demonstrated that using the large core diameter photonic crystal fiber amplifier for amplification of stretched pulses, a nonlinear impact of the Kerr effect can be significantly reduced, therefore the pulse characteristics required for the nonlinear frequency conversion can be achieved.

6. The research of the continuum generation in crystals with pulses from the femtosecond fiber laser operating at the 1 MHz repetition rate enables using this continuum radiation as a seed source of the optical parametric amplifier.

7. The utilization of a new BiBO crystal for amplification of the continuum allows one to create a wavelength tuning system based on the optical parametric amplifier pumped with low energy (~1 μJ) pulses at the 1 MHz repetition rate.

Statements to be defended

1. The use of a low dispersion (0.25 ps/nm) chirped fiber Bragg grating in a passively mode-locked fiber oscillator allows one to compensate normal dispersion of other cavity components and to generate close to transform-limited pulses with the duration of 380 fs that are suitable for the parabolic pulse generation.

2. The compensation of the third order dispersion introduced by the diffraction grating pulse compressor in fiber CPA system can be achieved by using of chirped fiber Bragg grating with optimized dispersion profile which makes it possible to generate high fidelity femtosecond pulses at the output of the system.

3. The distortion of linear chirp profile of pulse stretcher based on chirped fiber Bragg grating and chirped volume Bragg grating pulse compressor limits the temporal pulse quality at the output of the CPA system and only matching of

dispersion profiles of pulse stretcher/compressor allows one to improve temporal quality of compressed pulses.

4. The continuum generation in the 5 mm thick YAG crystal and continuum amplification in a 2 mm thick BiBO crystal allows one to generate femtosecond pulses in the range of 690 nm-2040 nm and to achieve the efficiency of >15 % in saturated regime using pump pulses with the energy of 1 μJ which were generated from fiber laser operating at 1 MHz pulse repetition rate.

Author's contribution

All the research presented in this thesis was performed in Laser Technology Department of Center for Physical Sciences and Technology as well as in Science and Technology Park of Institute of Physics and in the company EKSPLA during the period of 2013-2017. The author has constructed almost all described experimental setups, conducted measurements, analyzed experimental data with respect to numerical models and prepared publications. Co-authors' contribution is indicated in the following subsection.

Co-authors' contribution

- Dr. Andrejus Michailovas was a supervisor of the author's PhD studies, provided excellent conditions for the research and contributed to the preparation of scientific publications ,
- Dr. Nerijus Rusteika provided the most valuable ideas and consultation on various issues as well as strongly contributed to the preparation of scientific publications and this thesis ,
- Dr. Rokas Danilevičius provided a consultation on numerical simulation of fiber systems. He also shared his experience in the continuum generation and ultrafast optical parametric amplification topics.
- Tadas Bartulevičius contributed to the assembly of experimental schemes of the chirped pulse amplification in the photonic crystal fiber and made measurements
- Dr. Julijanas Želudevičius provided consultations on various issues of the fiber technology.
- Dr. Audrius Zaukevičius provided consultations on the continuum generation and carried out modeling of the continuum amplification.

Scientific papers

Scientific papers related to the topic of the thesis:

A1. **S. Frankinas**, T. Bartulevičius, A. Michailovas, N. Rusteika, „Investigation of all-in-fiber Yb doped femtosecond fiber oscillator for generation of parabolic pulses in normal dispersion fiber amplifier", Optical Fiber Technology, **36**, 366-369, (2017).
https://doi.org/10.1016/j.yofte.2017.05.012

A2. T. Bartulevičius, **S. Frankinas**, A. Michailovas, R. Vasilyeu, V. Smirnov, F. Trepanier, and N. Rusteika, „Compact fiber CPA system based on a CFBG stretcher and CVBG compressor with matched dispersion profilį", Optics Express **25**, 19856-19862 (2017).
https://doi.org/10.1364/OE.25.019856

A3. K. Michailovas, A. Baltuska, A. Pugzlys, V. Smilgevicius, A. Michailovas, A. Zaukevicius, R. Danilevicius, **S. Frankinas**, and N. Rusteika, „Combined Yb/Nd driver for optical parametric chirped pulse amplifiers", Optics Express **24**, 22261-22271 (2016).
https://doi.org/10.1364/OE.24.022261

A4. **S. Frankinas**, A. Michailovas, N. Rusteika, V. Smirnov, R. Vasilieu, A. L. Glebov, „Efficient ultrafast fiber laser using chirped fiber Bragg grating and chirped volume Bragg grating stretcher/compressor configuration", Proc. SPIE 9730, Components and Packaging for Laser Systems II, 973017 (2016).
doi: 10.1117/12.2214720

Conference presentations

<u>**Presentations directly related to the topic of the thesis:**</u>
Name of the presenting author is underlined.

C1.   <u>**S. Frankinas**</u>, R. Danilevičius, N. Rusteika, *High power femtosecond CPA system with TOD compensating chirped fiber Bragg grating strecher*, 16th International Conference "Laser optic 2014", St. Petersburg, Russia, June 30– July 4, 2014 (poster presentation).

C2.   **S. Frankinas**, <u>T. Bartulevičius</u>, R. Danilevičius and N. Rusteika, *Generation of Ultrashort Pulses from Passively Mode-Locked Yb Fiber Oscillator Utilizing Low Dispersion Chirped Fiber Bragg Grating*, 58th International Conference for Students of Physics and Natural Sciences "Open Readings 2015", Vilnius, Lithuania, March, 24-27, 2015 (poster presentation).

C3.   <u>**S. Frankinas**</u>, T. Bartulevičius, A. Michailovas and N. Rusteika, *Compact femtosecond fiber laser CPA system with tunable dispersion chirped fiber Bragg grating stretcher and chirped volume Bragg grating compressor*, The International Conference Northern Optics & Photonics "NOP 2015", Lappeenranta, Finland, June 2-4, 2015 (poster presentation).

C4.   <u>**S. Frankinas,**</u> T. Bartulevičius, A. Michailovas and N. Rusteika, *Skaidulinė femtosekundinė čirpuotų impulsų stiprinimo sistema su trečios eilės dispersijos kompensavimu panaudojant čirpuotą šviesolaidinę Brego gardelę*, 41-oji Lietuvos nacionalinė konferencija, Vilnius, Lithuania, June 17-19, 2015 (poster presentation).

C5.   <u>**S. Frankinas**</u>, A. Michailovas, N. Rusteika, V. Smirnov, R. Vasilyeu, A. L. Glebov, *Efficient ultrafast fiber laser using chirped fiber Bragg grating and chirped volume Bragg grating stretcher/compressor configuration*, International Conference "Photonic west 2016", San Francisco, USA, February 13-18, 2016 (poster presentation).

C6.   <u>T. Bartulevičius</u>, **S. Frankinas** and N. Rusteika, *High Power Femtosecond FCPA System Using ROD-type Photonic Crystal Fiber*, 59th International Conference for Students of Physics and Natural Sciences "Open Readings 2016", Vilnius, Lithuania, March, 15-18, 2016 (poster presentation).

C7.   <u>**S.Frankinas,**</u> A. Michailovas, N. Rusteika, *Looking for efficient compressor for high pulse energy femtosecond fiber laser*, 17th International Conference "Laser optic 2016", St. Petersburg, Russia, June 27– July 1, 2016 (oral presentation).

C8.   <u>**S. Frankinas**</u>, R. Danilevičius, N. Rusteika, *All-in-fiber Yb Doped Femtosecond Fiber Oscillator Based On Low Dispersion Chirped Fiber Bragg Grating*, 7th EPS-QEOD Europhoton Conference "Solid State, Fibre and Waveguide Coherent Light Sources", Vienna, Austria, August 21-26, 2016 (poster presentation).

C9.   <u>**S. Frankinas,**</u> T. Bartulevičius, A. Michailovas and Nerijus Rusteika, *Investigation of Passively Mode-locked Fiber Yb Doped Femtosecond Oscillator for Generation of Parabolic Pulses in Fiber Amplifier*, 60th

International Conference for Students of Physics and Natural Sciences "Open Readings 2017", Vilnius, Lithuania, March, 14-17, 2017 (poster presentation).

C10. **S. Frankinas**, T. Bartulevičius, A. Michailovas, *Pasyvios modų sinchronizacijos iterbio femtosekundiniai skaiduliniai lazeriai spinduliuotės dažnio keitimui panaudojant netiesinius procesus*, 42-oji Lietuvos nacionalinė konferencija, Vilnius, Lithuania, October 4-6, 2017 (oral presentation).

Other presentations at conferences:

C11. **S. Frankinas**, N. Rusteika, *3W femtosecond high repetition fiber laser,* XXth Lithuania-Belarus seminar "Lasers and Optical Nonlinearity", Vilnius, Lithuania, November 21-22, 2013, (poster presentation).

C12. V. Vosylius, M. Safinas, K. Viskontas, **S. Frankinas**, N. Rusteika, R. Danilevičius, A. Michailovas, *All in Fiber Chirped Pulses Picosecond Laser Prototype for Seed Synchronization of Yb and Nd Lasers*, XXth Lithuania-Belarus seminar "Lasers and Optical Nonlinearity", Vilnius, Lithuania, November 21-22, 2013, (poster presentation).

C13. **S. Frankinas**, N. Rusteika, and A. Michailovas, *Compact high repetition rate femtosecond optical parametric generator and amplifier pumped by femtosecond Yb fiber laser,* CLEO®/Europe-EQEC 2017, Munich, Germany, June 25-29, 2017 (poster presentation).

Thesis summary

The thesis consists of 5 chapters, conclusions and a list of references. The thesis is presented in 126 pages, contains 66 figures and 3 tables.

Chapter 1: Literature review

This chapter consists of 2 subchapters. In subchapter 1.1, tunable ultrashort pulse laser sources are reviewed. One of the main methods based on the optical parametric amplification (OPA) that allows ones extend the tenability of the ultrashort pulse laser is described. Moreover, the applications of tunable laser sources and requirements for biological imaging – two and three photon microscopies - are reviewed in this subchapter. Also, in this subchapter, the advantages of fiber lasers against solid state laser sources are discussed.

The combination of ytterbium fiber lasers and the optical parametric amplification could allow developing compact and tunable femtosecond pulses laser systems for biomedical applications. However, a high intensity of pulses for the pump OPA is required. The generation of such pulses in fiber laser systems is not simple due to the nonlinear effect in fibers arising due to strong light confinement in the fiber core. Therefore, in subchapter 1.2, the main techniques – the chirped pulse amplification (CPA) and the fiber diameter scaling - for the ultrashort pulse generation in the fiber laser are reviewed. Various configurations of the pulse stretcher/compressor in fiber CPA systems are also reviewed.

Chapter 2: Controlling of pulse spectral and temporal characteristics in the fiber oscillator

In this chapter, a method for manipulation of pulse spectral and temporal characteristics in a passively mode-locked fiber oscillator is presented. The described method is based on modification of characteristics of the chirped fiber Bragg grating (CFBG) that is used in the cavity. First of all, the operation of the passively mode-locked fiber oscillator is described. Secondly, the dependence of the generated pulse duration on the cavity dispersion is discussed. Lastly, the method for spectral filtering of Kelly sidebands, that are common in the pulse spectrum, is presented.

The layout of the passively mode-locked fiber oscillator is illustrated in Fig.1. The pulses were generated in the linear cavity consisting of CFBG, the Yb doped fiber, the beam splitter and the semiconductor saturable absorber mirror (SESAM). The Yb doped fiber was in the core pumped with the single mode laser diode at the 976 nm wavelength. The polarizing beam splitter with the polarization extinction ratio of 22 dB was used as the cavity out-coupler. CFBG has a couple of functions. Firstly, it acted as the end mirror of the cavity and formed the pulse spectrum. Secondly, CFBG was an anomalous dispersion source in the cavity that compensates normal dispersion of the cavity consisting of the silica fiber. The back mirror of the cavity was a SESAM coupled to the resonator by the optical contact to the fiber. SESAM was used to ensure self-starting of the mode-locking process and stabilization of the solitary pulse against perturbations. The combining of a fiber-coupled SESAM as a mode-locker and a CFBG for dispersion control allows one to realize a compact,
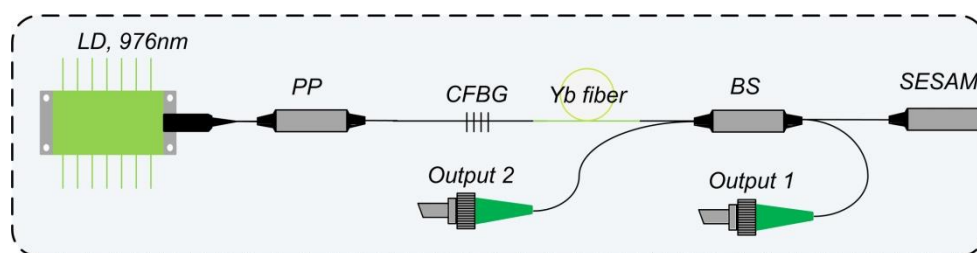

Fig. 1. A principal scheme of passively mode-locked fiber oscillator used in the study.

environmentally stable all-in-fiber design of the oscillator. In this work oscillators which generate pulses at the $30 - 70$ MHz repetition rate were demonstrated. The pulse repetition rate was varied by changing the amount of passive fiber in the cavity. The stable self-starting single pulse mode-locking regime from the fiber oscillator was obtained by increasing the pump power. The typical spectral profile of the oscillator output in the stable single pulse regime is plotted in Fig.2. In the recorded spectrum Kelly sidebands – typical of soliton pulses [19,20] – are also visible. It is important to mention that these pulses are not the same as real solitons, that propagate long distances without temporal and spectral changes [21]. This design of the oscillator cavity has a

non-uniform dispersion map (normal and anomalous dispersion), therefore the temporal envelope and the spectral shape of generated pulses vary along the cavity but recur after the full cycle. Such pulses are known as average solitons [19,20]. When the pump power is increased beyond the mode-locking self-starting threshold, more pulses are obtained s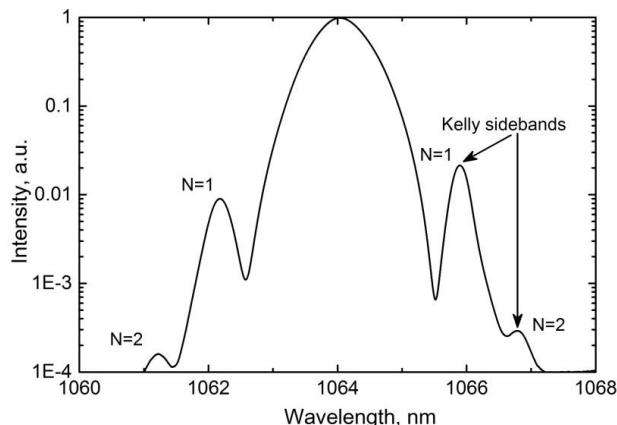imultaneously in the cavity. These pulses circulate in the cavity and exhibit complex relative temporal movements. However, this operation regime of the fiber oscillator is not used in practice.

Fig.2. A typical spectral profile of the passively mode-locked fiber oscillator in the stable single pulse regime.

The impact of the total cavity dispersion value and sign on pulse dynamics in the passively mode-locked fiber oscillator were described in this work [19]. The duration of oscillator pulses depends on the total cavity dispersion that can be varied by changing the distance between diffraction gratings. The use of CFBG instead of diffraction gratings drastically simplifies the oscillator scheme. Despite the fact that dispersion of CFBG is fixed, from a practical point of view the compactness and reliability of the oscillator are more preferred. Nowadays CFBG writing technology is sufficiently well developed and allows realizing various dispersive and spectral characteristics of CFBG. However, one of the main limitations of this technology is that the reflection of CFBG decreases reducing the dispersion. For this reason, the achievable dispersion of CFBG is limited; therefore, the pulse duration from the oscillator cannot be very short. Therefore, one of the tasks of this work was to generate pulses shorter than 1 ps from the fiber oscillator using the low dispersion CFBG. The principal optical scheme of fiber oscillators is the same as shown in Fig.1. Characteristics of the used CFBG were summarized in Table 1. In order to ensure self-starting of the mode-locking process the SESAM that had the reflectivity modulation depth of 37 % and the relaxation time of around 15 ps was used. Measurements of the pulse duration were performed by using the second harmonic autocorrelator (EKSPLA) at the same level that was under the mode-locked threshold. Despite a high loss in the oscillator due to the low reflection of CFBG the stable self-starting mode-locking was obtained at the 40 MHz repetition rate with the chosen CFBG. The measured pulse duration and energy are listed in Table 1. Using CFBG with the dispersion of 0.25-0.82 ps/nm the oscillator generates 0.48-1.2 ps pulses. Summarizing experimental results, it can be concluded that the duration of oscillator pulses decreases when reducing the dispersion of CFBG. As can be seen from

Table 1. The characteristics of CFBG used in experiments and pulse parameters of generated pulses at the 40 MHz repetition rate.

D_{CFBG}, ps/nm	R,%	λ_c, nm	τ, ps	E, pJ
0.82	50	1030	1.2	110
0.62	30	1030	1	88
0.42	20	1064	0.75	24
0.25	19	1064	0.48	14

Table 1 the shortest pulse duration (480 fs) was obtained using the 0.25 ps/nm dispersion of CFBG. In this case the dispersion of the CFBG was comparable to the dispersion of the passive fiber in the cavity with the opposite sign, therefore spectral and temporal characteristics of the pulses were dependent on the pulse repetition rate of the oscillator. This can be clearly seen in Fig.3a. The repetition rate was varied by changing the amount of the passive fiber in the cavity, which also affected the total cavity dispersion. When lowering the repetition rate, TCD as well as the pulse duration also decreased. The spectral bandwidth increased accordingly. The stable self-starting single pulse mode-locking regime from the fiber oscillator was obtained in the 32–72 MHz repetition rate range. The shortest pulse duration was obtained at the 32 MHz repetition rate. The measured autocorrelation trace of the pulses is shown in Fig. 3b. Assuming the Gaussian shape the pulse duration was 380 fs at full width of half maximum (FWHM). The spectral profile of the pulses was measured by an optical spectrum analyzer and is plotted in the inset of Fig. 3b. The spectrum had the FWHM bandwidth of 5.2 nm and was close to the Gaussian spectral shape. In the recorded spectrum, Kelly sidebands –
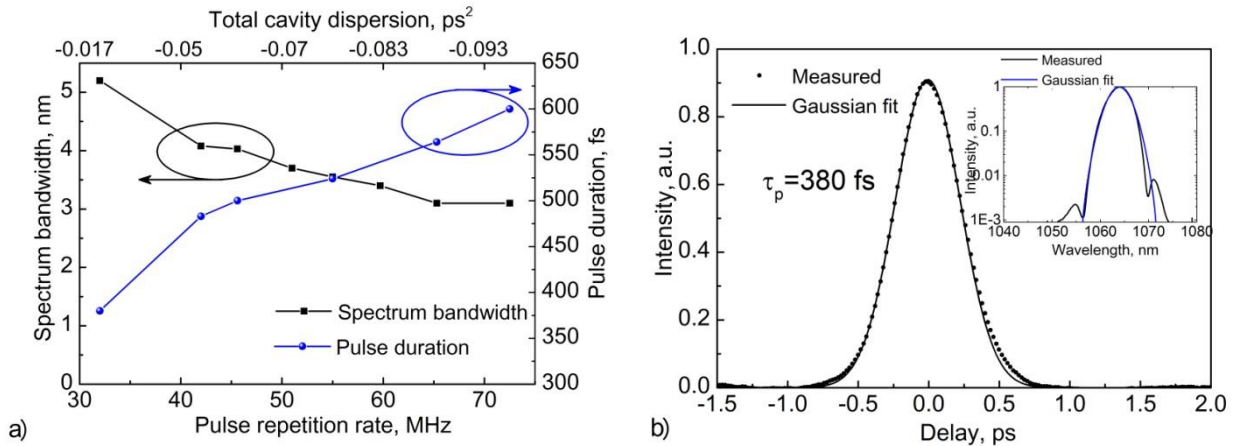

Fig.3. a) Measured dependences of the pulse bandwidth and the pulse duration on the repetition rate/total cavity dispersion; **b)** measured autocorrelation trace of oscillator pulses and optical spectrum (inset) at the 32 MHz repetition rate.

typical of soliton pulses – were also visible. The spectral amplitude of Kelly sidebands is lower by 20 dB compared to the main peak. This is due to the spectral filtering of the CFBG in the resonator. Reduction of the amplitude of Kelly sidebands is important for using the pulses in the nonlinear FCPA system as the interference of this sharp spectral feature with the main peak will cause modulations of the spectrum.

Lastly, numerical simulations were performed in order to demonstrate the method that reduces the intensity of Kelly sidebands, which are common in the pulse spectrum. The oscillator that uses the 0.62 ps/nm dispersion was chosen for simulation. Simulated pulse spectra at a different reflection bandwidth of CFBG both with normalized reflection profiles of CFBG are shown in Fig.4a. In both cases Kelly sidebands are under the reflection profiles of CFBG, however, in the case of a narrower CFBG the first Kelly sideband is quite intensive. The intensity of this sideband can be strongly reduced by narrowing the reflection bandwidth of CFBG. This can be clearly seen in Fig.4a where the simulated pulse spectrum at the 5 nm reflection bandwidth CFBG is shown. The intensity ratio of the Kelly sideband compared with the main part of the pulse increases from 1:20 up to 220:1. It is important to mention that reducing the reflection bandwidth of CFBG two times does not affect the pulse duration, therefore
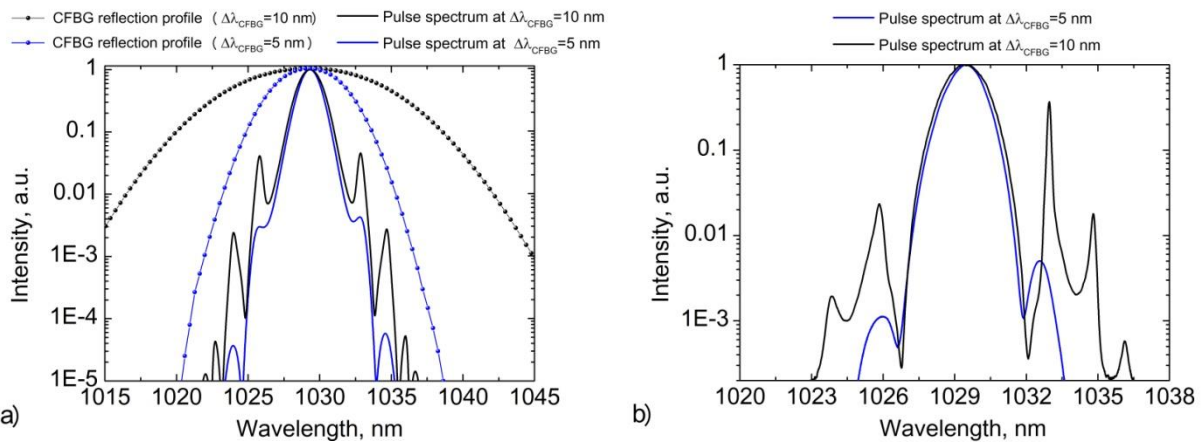

Fig. 4.a) Numerical simulation of spectral profiles of oscillator pulses generated using CFBG that had reflection bandwidth of 10 nm and 5 nm and reflection profile of CFBG used in simulation; **b)** measured spectral profiles of oscillator pulses generated using CFBG with a different reflection bandwidth.

the pulse duration remains to be about 1 ps. These numerical simulations were confirmed by experimental results. Oscillators, which use CFBGs with the reflection bandwidth of 10 nm and 5 nm, were assembled. The pulses at the 40 MHz repetition rate were generated and all measurements were performed at the same level. Measured pulse spectra of these oscillators are shown in Fig.4b. As expected the intensity of the Kelly sideband in the pulse spectrum was reduced by using a narrower CFBG. The narrowing of the CFBG reflection bandwidth had a minimal impact on the pulse duration – the pulse duration increased from 0.93 ps to 1 ps.

Chapter 3: Controlling of pulse spectral and temporal characteristics in fiber chirped pulse amplification systems

In this chapter methods for manipulation of pulse spectral and temporal characteristics in the fiber chirped pulse amplification (CPA) systems are discussed. These methods are based on the use of various combinations of the pulse stretcher/compressor. Firstly, the pulse stretching and compression in the fiber CPA system that uses the chirped fiber Bragg grating (CFBG) stretcher and the diffraction grating compressor are discussed. After that a novel CPA system consisting of the CFBG with tunable dispersion as a pulse stretcher and the chirped volume Bragg grating (CVBG) as a pulse compressor is presented. The main purpose of the study of these CPA systems was to determine the possibilities and limitations of different pulse/stretcher configurations of developing new fiber lasers that generate high fidelity femtosecond pulses. Finally, methods for the pulse spectral modification in fiber lasers is described.

Chapter 3.1: Fiber CPA system based on the CFBG stretcher and the diffraction grating pulse compressor

A principal optical scheme of the fiber CPA system based on the CFBG stretcher and the diffraction grating compressor is illustrated in Fig. 5. The initial pulses of the 2 ps duration and the 50 pJ energy were generated in the passively mode-locked fiber oscillator. The oscillator pulses were amplified in a single mode Yb doped fiber amplifier and were propagated through ~50 m of the single mode passive fiber used to
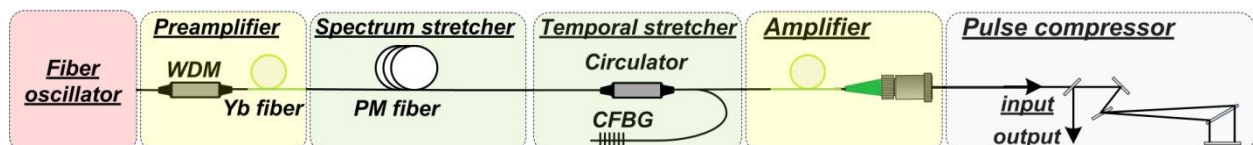

Fig.5. A principal optical scheme of the fiber CPA system.

broaden the pulse spectrum. The pulse spectrum was broadened in the passive fiber due to self-phase modulation caused by the nonlinear Kerr effect. The bandwidth of the pulse spectrum after the after the passive fiber depends on the initial pulse energy. This pulse spectrum spreading enables achieving femtosecond pulses at the end of the system. Spectrally broadened pulses were directed to the CFBG stretcher through the three port circulator. Stretched pulses were amplified in the single mode Yb doped amplifier and compressed using a pair of diffraction gratings. In order to achieve high fidelity femtosecond pulses at the output of the system the second and third order of the group velocity dispersion between the pulse stretcher and the compressor should be matched. However, in the fiber CPA system that used the pulse stretcher/compressor based on different technology the third order dispersion (TOD) is not compensated automatically

by matching the second order dispersion. Therefore, firstly it was decided to investigate the impact of uncompensated TOD on the pulse compression using a numerical simulation. The CFBG with dispersion of 12.5 ps^2 was used to stretch pulses of the 3.5 nm bandwidth to the 80 ps duration. Stretched pulses were compressed down to the 600 fs duration using diffraction gratings that had 1000 grooves per mm. The simulated temporal envelope of compressed pulses is shown in Fig.6a. It can be clearly seen that almost all of the pulse energy is located in the main pulse. To compare the quality of compressed pulses with other CPA systems a parameter of temporal contrast was introduced. This parameter shows what part of the pulse energy is located in the main pulse. This parameter is the ratio of the Gaussian fit of the temporal envelope and the temporal envelope areas. In this case 96.8 % of the pulse energy is in the main part of the
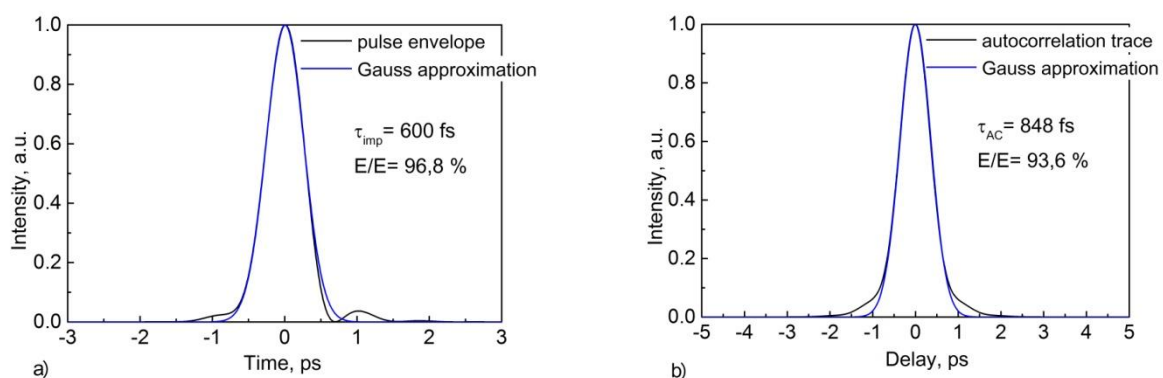

Fig.6. Numerically calculated envelope (a) and autocorrelation trace (a) of pulses at the output of the fiber CPA system.

pulse (Fig.6a). This evaluation of the pulse temporal quality method is practical in performing a numerical simulation of the system. In case when optimization of the CPA system is performed experimentally an autocorrelation trace of the compressed pulse (trace) is measured. In this context it is more practical to compare the measured autocorrelation with the Gauss approximation. The temporal pulse contrast in this case is the ratio of the area of the Gauss approximation and the measured autocorrelation trace. Using this calculation procedure, it was obtained that 6.4 % of the pulse energy was out the main part of the pulse (Fig. 6b). In conclusion, the temporal quality of compressed pulses can be estimated from measured autocorrelation traces but it should be borne kept in mind that the real amount of the pulse energy on the uncompressed pedestal is two times less.

A numerical simulation of the described CPA scheme showed that high fidelity pulses could be obtained without the TOD compensation. However, the pulse compressor that used diffraction gratings of 1000 gr/mm to compress stretched pulses of the 80 ps duration was not compact. In this case the distance between gratings was 2.25 m. On the other hand, a larger pulse stretching is required in real fiber CPA systems to suppress nonlinearity of the fiber amplifier. Therefore, increasing the distance

between gratings also increases TOD introduced by the compressor. This can be seen from numerical simulation of the system at which stretched pulses of the 80 ps, 100 ps, 200 ps and 300 ps duration were compressed. Calculated envelopes of compressed pulses (Fig.7 a) showed that the duration of compressed pulses slightly increased and the pulse energy of the main pulse slightly decreased. This can be attributed to the increasing
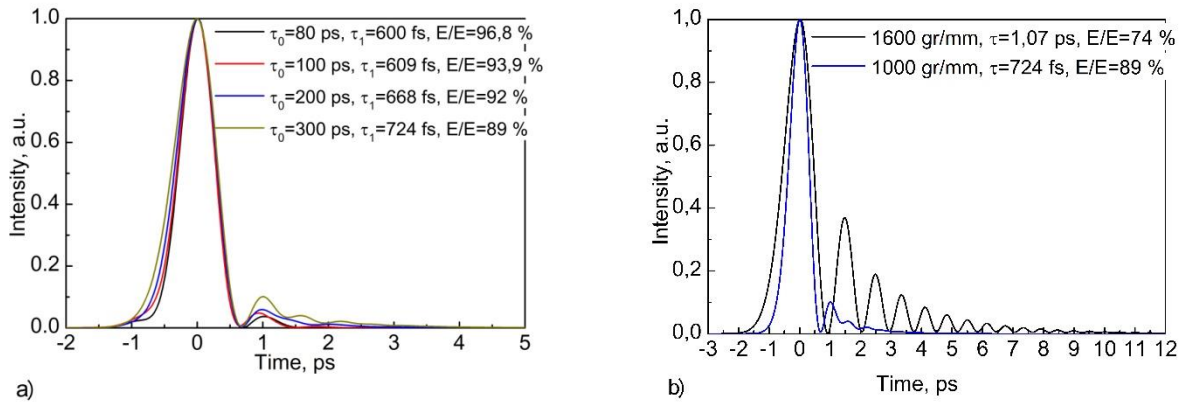

Fig. 7.a) Numerically calculated envelopes of compressed pulses using 1000 gr/mm gratings while initial pulses of the system were stretched to different durations (τ_0), τ_1-duration of compressed pulses; **b)** numerically calculated envelopes of compressed pulses using 1000 gr/mm and 1600 gr/mm diffraction grating compressors.

uncompensated TOD introduced by the pulse compressor. To reduce the footprint of the pulse compressor the gratings with a higher density of grooves are used. The geometrical size of 1600 gr/mm of the diffraction grating compressor decreases drastically, however a larger amount of TOD is introduced. This was confirmed by numerical simulation of the system and the results are shown in Fig.7b. The compression of stretched pulses of the 300 ps duration using 1600 gr/mm gratings was modeled. Calculated envelopes of compressed pulses (Fig.7 b) showed that the duration of compressed pulses was larger than previous case. Also the energy part outside of the main pulse was increased. This can be attributed to increasing of the uncompensated TOD introduced by the pulse compressor.
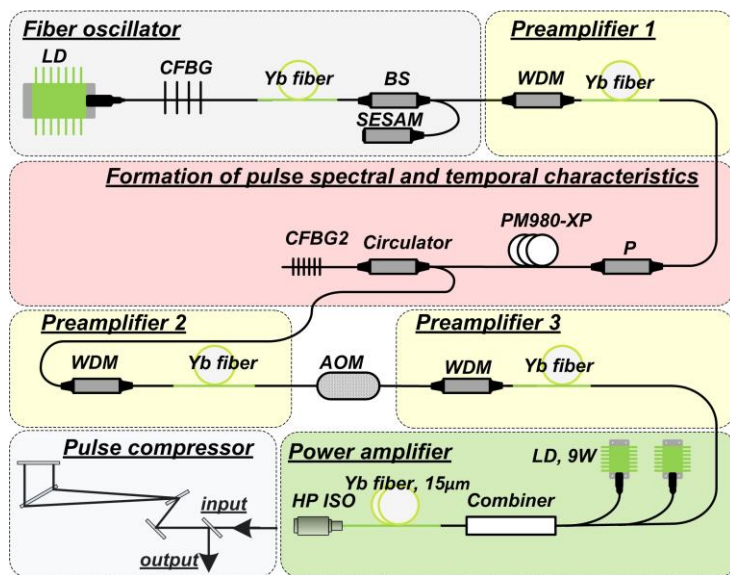
To improve the temporal quality of compressed pulses in a compact CPA system the compensation of TOD should be performed. In this work the compensation of TOD was realized using the same CFBG that was used as a

Fig. 8. A principal optical scheme of fiber CPA system with TOD compensation.

pulse stretcher. Nowadays technologies of the Bragg grating writing in the fiber core enables one to achieve not only required GVD, but also the TOD value that opens up opportunities to compensate TOD introduced by the compressor. To demonstrate this dispersion matching principle a fiber CPA system (Fig.8) was assembled. The spectrum of initial pulses was stretched to 7.5 nm in the passive fiber. Spectrally broadened pulses were directed to the CFBG stretcher through the three port circulator. CFBG had dispersion of 24.88 ps^2, therefore pulses were stretched to 350 ps.

Fig. 9. Measured autocorrelation trace of compressed pulses at 4 µJ energy (black curve); numerically calculated autocorrelation traces of compressed pulses for different cases: without TOD compensation (green curve), with TOD compensation (blue curve) and with TOD compensation but without amplification in the power amplifier (red curve).

Moreover, TOD of the stretcher was matched to the diffraction grating pulse compressor. In the fiber CPA system the pulse repetition rate was reduced to 1 MHz by an acousto-optic modulator. Two preamplifier stages were used to increase the pulse energy suitable for the power amplifier consisting of the double clad Yb doped fiber with the core diameter of 15 µm. The power amplifier was pumped by two multimode diodes which emit the 9 W average power at the 976 nm wavelength. Stretched pulses were amplified up to the 4 W average 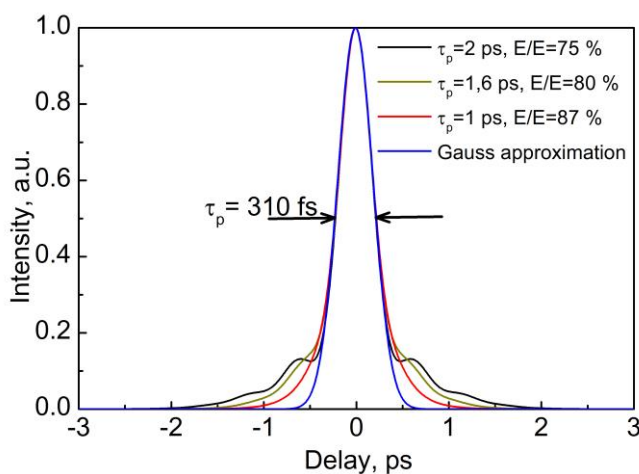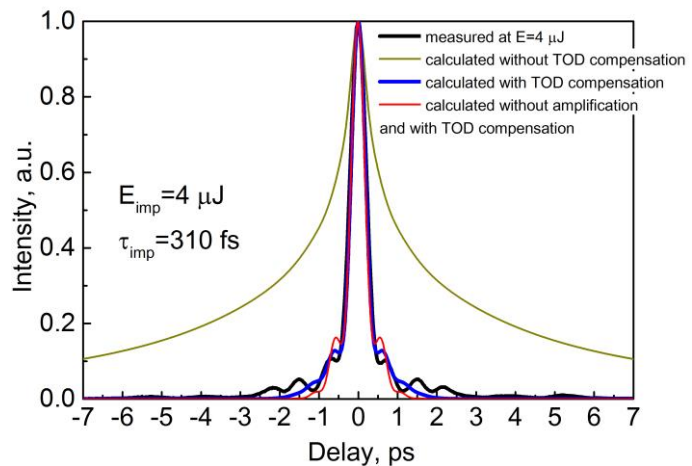power (4 µJ) and compressed down to 310 fs using diffraction gratings of 1600 gr/mm. The measured autocorrelation trace of compressed pulses (black curve) in comparison with the calculated one (blue curve) is shown in Fig.9. Good agreement between experimental and simulation results was obtained. For comparison the autocorrelation trace of pulses at the output of the system without TOD compensation is also shown in Fig. 9 (green curve). It can be seen that the temporal quality of pulses at the output is very poor –

Fig. 10. Calculated envelopes of compressed pulses when initial pulses of 1 ps, 1.6 ps and 2 ps were used in the system.

most of the energy is concentrated on the pedestal of the 60 ps length. As was assumed, the compensation of the compressor TOD significantly improves the pulse temporal quality at the output of the CPA system. However, even in this case, when TOD is compensated, the temporal quality of compressed pulses is not ideal. A numerical calculation of compression of pulses before the power amplifier was performed (red curve). The calculated autocorrelation trace has shown that ~15 % of the pulse energy is out of the main pulse. This result means that the nonlinear phase is accumulated in the passive fiber broadening pulse spectrum and that limits the pulse quality. In order to reduce distortion of the pulse chirp shorter initial pulses can be used. This was confirmed by a numerical calculation of the CPA system while the duration of initial pulses was 2 ps, 1.6 ps and 1 ps. As can be seen from calculated autocorrelation traces of compressed pulses (Fig. 10) the best quality of pulses at the output was achieved using initial pulses with the duration of 1 ps. This result is very important in the high energy femtosecond fiber systems.

Chapter 3.2: Fiber CPA system based on the tunable CFBG stretcher and the fixed dispersion CVBG compressor

In this chapter a novel chirped pulse amplification configuration consisting of the chirped fiber Bragg grating with tunable dispersion as a pulse stretcher and the chirped volume Bragg grating as a pulse compressor is presented. The optical layout of the fiber CPA system investigated in this work is shown in Fig. 11. The seed source of the system is a passively mode-locked all-in-fiber picosecond oscillator, operating at the 1030 nm central wavelength. In the stable mode-locking regime the oscillator generated nearly bandwidth-limited pulses with the duration of 1.6 ps and 40 pJ at the 40MHz repetition rate. Pulses from the oscillator were amplified in a single mode Yb doped fiber amplifier which is spliced to ~50 m of the single mode passive fiber used to broaden the pulse spectrum. The broadened pulse spectra of different energy are shown in Fig.12a. Temporal shapes of stretched pulses were measured using a fast photodiode (16 ps response time) and a fast real-time oscilloscope (20 GHz bandwidth). Measured stretched pulse durations
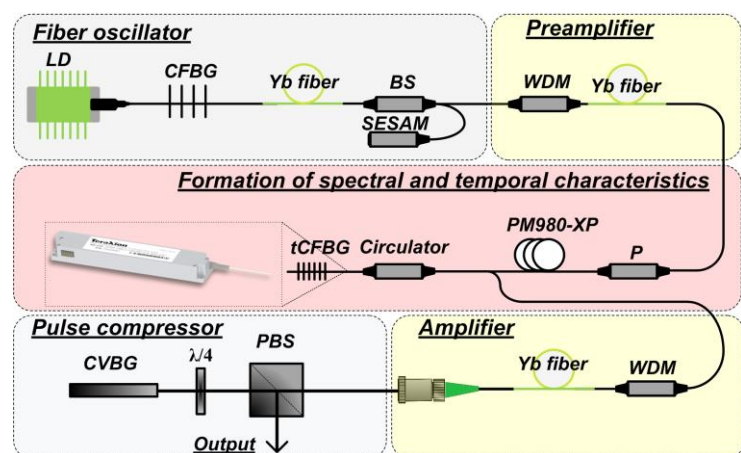

Fig.11. A principal optical scheme of fiber CPA system with the tunable dispersion pulse stretcher and fixed dispersion pulse compression.
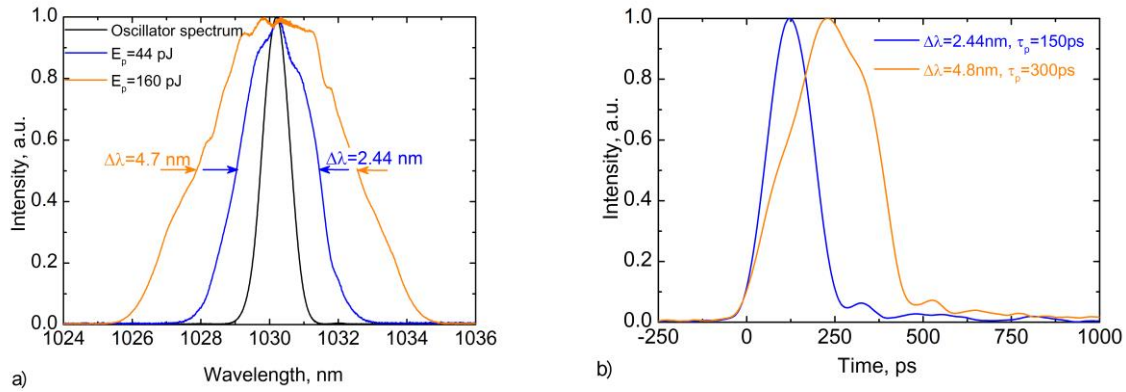
Fig.12.a) Measured pulse spectrum from the oscillator and after spectral broadening in the 50m single mode fiber for two different pulse energies; **b)** oscilloscope traces of the stretched pulses after CFBG.

were 300 ps for the 4.8 nm bandwidth pulses and 150 ps for the 2.4 nm bandwidth (Fig. 12b). To facilitate further measurements stretched pulses were amplified in an additional single mode Yb doped amplifier up to 40 mW. As the main purpose of this study was to demonstrate a principle of dispersion matching between a novel combination of the tunable CFBG stretcher and the CVBG compressor we did not use a high power amplifier. To compress the pulses the 49 mm long CVBG with an 8.8 nm bandwidth centered at 1030 nm (with a square input aperture of 5 * 5 mm), recorded in photo-thermal refractive (PTR) glass, was used. Optimization of the pulse compression was performed by thermally tuning the dispersion of the CFBG stretcher. The duration of compressed pulses was measured by a second harmonic autocorrelator (*Ekspla*). The dependence of the measured pulse duration on the stretcher dispersion (Fig. 13a) shows that the stretcher and the compressor GVD were matched at the 62.7 ps/nm dispersion of the CFBG stretcher. The autocorrelation trace of the optimally compressed pulses is shown in Fig. 13b. The achieved pulse duration was 910 fs with the pulse bandwidth of 2.44 nm that corresponds to transform-limited pulse duration of ~640 fs. By increasing the spectrum bandwidth in the system, the shorter duration of compressed pulses was obtained, however a significant deterioration in the pulse quality was observed. The
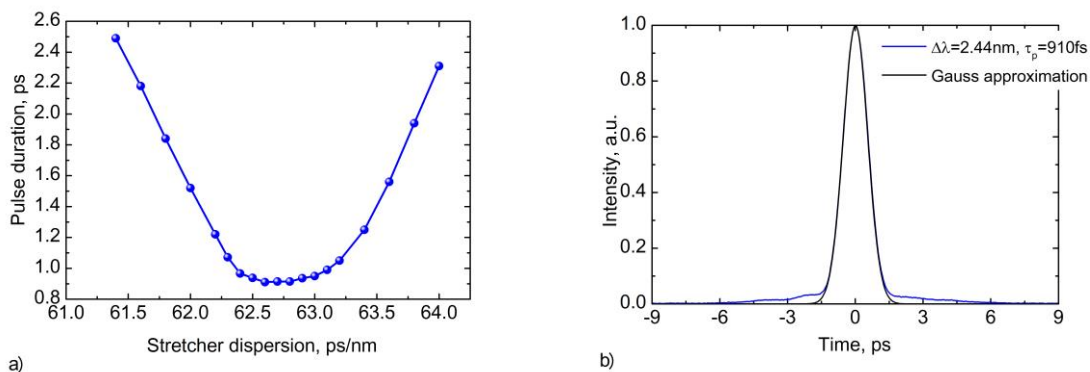

Fig.13.a) A dependence of the measured pulse duration on the stretcher dispersion; **b)** the measured autocorrelation trace of pulses at the output of the femtosecond fiber laser CPA system for the 2.44nm bandwidth.

comparison of the autocorrelation traces of compressed pulses with a different bandwidth is presented in Fig. 14. The shortest achieved pulse duration was ~750 fs (red curve) with the bandwidth of 4.8 nm (corresponds to transform-limited ~320fs pulses). However, pulses of this bandwidth possessed a larger remaining picosecond pedestal after the compression compared to the 910 fs 2.44 nm bandwidth pulses (blue curve). The un-compressed pedestal as well as deviation from the transform-limited pulse duration may be attributed to the high order dispersion of either CFBG or VBG that could not be compensated by a simple thermal gradient on CFBG.
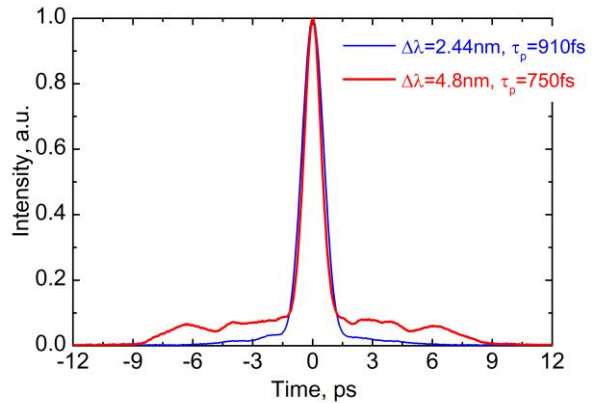

Fig. 14. The measured autocorrelation trace of pulses at the output of the femtosecond fiber laser CPA system for two different bandwidths.

The mismatch of dispersion profiles between the stretcher and the compressor is a typical problem in conventional CPA systems. The CPA system using the single CVBG as a pulse stretcher and a compressor eliminates pulse distortions associated with the dispersion mismatch. To verify this, the experiment of pulse stretching and recompression using the same CVBG was performed. The experiment
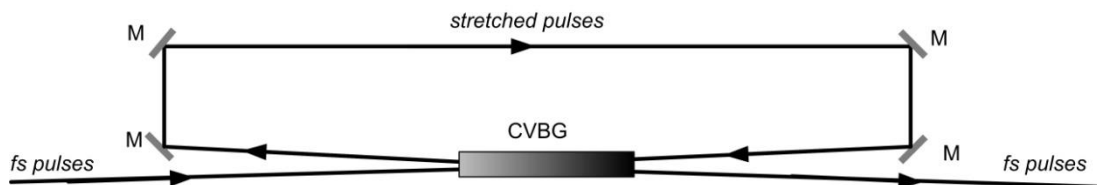

Fig.15. The experimental setup of pulse stretching and compression using a single CVBG.

setup is shown in Fig. 15. The pulses with the duration of 400 fs from the fiber laser were stretched to ~300 ps and recompressed back using the same CVBG. A small incidence angle to the CVBG was used to separate the reflected pulses from the incident pulses at both stretching and compressing parts. Incident angles of the beams were set to be equal. The longer duration of the recompressed pulses (570 fs) compared to the initial pulses (400fs) was observed (Fig.16.), which indicates the intrinsic minimal pulse duration achievable for the CVBG of this design. However, the temporal contrast achieved in the CVBG stretcher/ compressor configuration
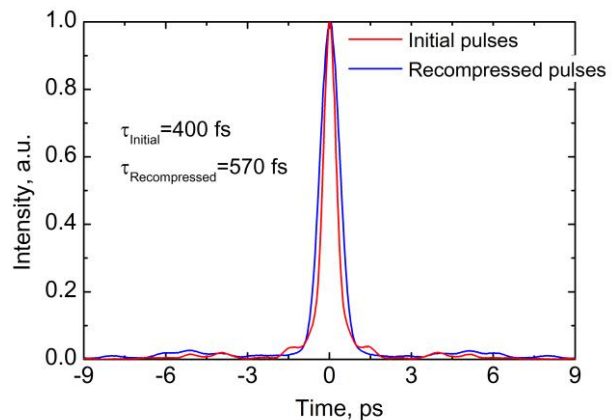

Fig. 16. The measured autocorrelation traces of initial and recompressed pulses using CVBG for stretching and compressing

(80 %) was better compared to the CFBG/CVBG pair confirming the hypothesis of the dispersion profile mismatch between CFBG and CVBG.

Compressed pulses of the fiber CPA system with the CFBG/CVBG pair were not transform-limited and had a temporal pedestal due to the imprecise dispersion compensation between CFBG and CVBG. In order to achieve high fidelity femtosecond pulses CFBG and CVBG with matched dispersion profiles should be used. In close cooperation with manufacturers of CFBG and CVBG (*TeraXion* and *OptiGrate*) the CFBG/CVBG pair with the matched dispersion profile was produced. The suitability of those dispersive elements for the fiber CPA system has been verified using the CPA system which is described in a publication [22]. The seed source of this system was the commercially available all-in-fiber passively mode-locked laser (FFS100CHI, *Ekspla*) that generates linearly up-chirped pulses of the 13 ps duration and the 10.6 nm bandwidth at the ~1030 nm center wavelength and the 53 MHz repetition rate. Pulses from the seed source were stretched to about the 230 ps duration by using the CFBG stretcher with the group velocity dispersion of -13.65 ps^2. Stretched pulses were amplified up to the 4.85 nJ energy and compressed in a free space with the CVBG compressor. Optimally compressed pulses were further characterized using the second harmonic generation (SHG) frequency-resolved optical gating (FROG) autocorrelation method. The pulse duration retrieved by the FROG algorithm (*Swamp Optics*) was equal to 208 fs, which is close to the transform-limited pulse duration (203 fs) derived from the spectrum. A close match between the transform-limited and retrieved pulse duration proves that the CFBG dispersion profile was successfully matched to that of CVBG.

Chapter 3.3: Controlling of pulse spectral characteristics in fiber lasers

In this chapter modification of the pulse spectrum in fiber systems is presented. In the previously described fiber CPA systems to preserve a smooth shape of the broadened pulse spectrum, a low pulse energy (<0.5 nJ) and a long length (~50 m) of the passive fiber were used. In this case the pulse spectrum has been broadened up to 10-12 nm at FWHM that enables one to achieve the 250-300 fs pulse duration at the system output (Fig.17a). Otherwise, when it is not necessary to maintain uniformity of the broadened spectrum the pulse spectrum can be broadened more using a larger energy of initial pulses (~2 nJ) and the short fiber (several meters). In this case the pulse spectrum poses a modulation and is wider than in the previous case (Fig. 17b). Different spectral regions of the broadened spectrum can be separated. This method was applied to create a dual output fiber oscillator/power amplifier to seed and assure the all-optical synchronization of the femtosecond Yb and picosecond Nd laser amplifiers operating at a central wavelength of 1030 nm and 1064 nm, respectively. The optical scheme of the dual output laser is discussed in more detail in publication [23].
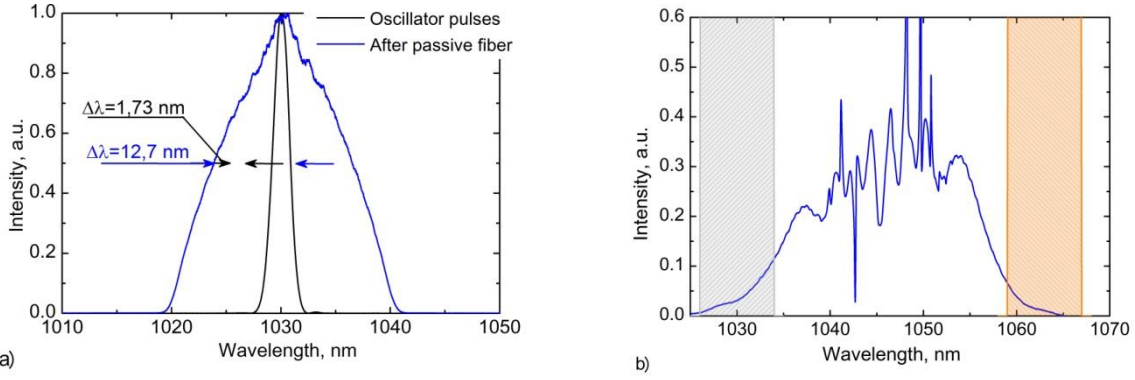
Fig.17. Pulse spectrum in fiber systems for different cases: **a)** low pulse energy (<0.5 nJ) and long length of passive fiber (~50 m); **b)** higher pulse energy (1.8 nJ) and short length of passive fiber (2 m).

Broadening of the pulse spectrum is possible not only in a passive fiber but also in the Yb doped fiber during the pulse amplification. When certain values of the pulse energy and the duration in conjunction with the parameters of the amplifier are chosen properly, a linearly chirped pulse with a parabolic shape can be generated due to interplay of normal dispersion, nonlinearity (self-phase modulation) and gain [24]. These pulses have the following features. Firstly, the temporal and spectral shapes of those pulses are maintained during a nonlinear propagation through the fiber, though the duration and the spectrum bandwidth of pulses increase due to dispersion and self-phase modulation. Secondly, pulses with a parabolic shape have a linear chirp that can be efficiently removed, allowing a high-quality pulse compression. Finally, parabolic pulses can be propagated in the fiber at a high peak power accumulating large B integral values (up to 5p) and still be recompressed to high fidelity femtosecond pulses, which cannot be achieved if the initial pulse shape is e.g. Gaussian [25]. The experimental realization of
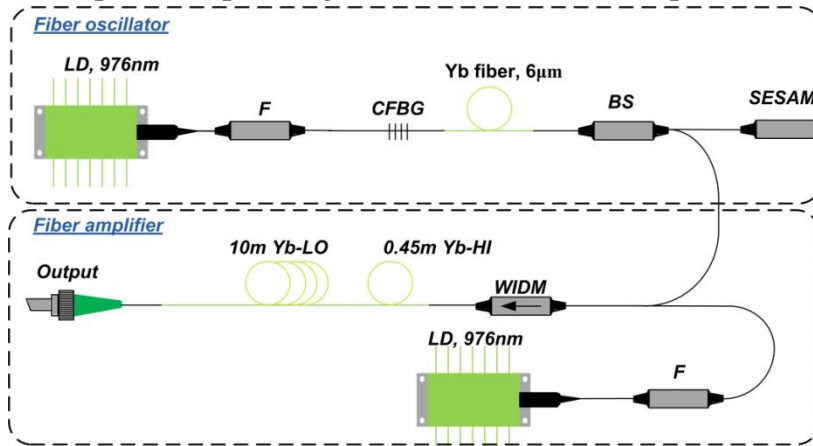

Fig.18. The layout of experimental setup consisting of the femtosecond passive mode-locked fiber oscillator and the parabolic fiber amplifier.

the parabolic fiber amplifier is shown in Fig.18. The previously described (Chapter 2) femtosecond passively mode-locked fiber oscillator generating pulses with the duration of 380 fs was used for the generation of chirped parabolic pulses in the fiber amplifier. Pulses from the oscillator were amplified in the polarization maintaining fiber amplifier that consisted of two gain fibers with the different Yb concentration. The first fiber (Yb-

HI) was highly Yb doped and it was used to boost the energy of the oscillator pulses up to 140 pJ without changing its spectral and temporal shape. The length of this fiber (0.45 m) was optimized to obtain parabolically shaped pulses from the output of the laser. Afterwards pulses were further amplified in the second fiber (Yb-LO) with the low Yb concentration. The length of this fiber was chosen to be 10 m and was fixed in the experiments. The preamplified pulses due to cumulative action of amplification, nonlinearity and dispersion, when propagating in the Yb-LO fiber, were parabolically shaped. After the fiber amplifier, the output pulses had the energy of 1.4 nJ, the duration of 6.5 ps and the spectral bandwidth of 22.8 nm. The measured pulse spectrum is shown in Fig. 19 (black color). The shape of the spectrum was close to parabolic with typical steep edges. A slight bump on the short wavelength side is due to the amplified spontaneous emission which has a peak at the gain maximum (1030 nm) of the Yb doped fiber. In addition to the experiments, numerical simulation of the parabolic amplifier was carried out by solving the nonlinear Schrodinger equation (NLSE) using the split-step Fourier method [26]. The simulated spectral profile is given along with the measured one in Fig. 19 (blue color). A minor discrepancy between the measured and simulated spectrum is due to the fact that initial pulses in our model had a perfect Gaussian shape while pulses from the oscillator may slightly deviate from that shape. The simulated temporal profile of pulses at the output of the fiber amplifier is close to the parabolic shape and pulses have a linear chirp (right hand scale in Fig. 19). The linear chirp of the pulses is a feature of parabolic propagation. It should get a result of the highly fidelity transform limited pulses after compression using a simple linear compressor (e.g. prism or grating pair). The calculated envelope of the transform limit of generated parabolic pulses is shown in the Inset of Fig. 4. The transform limited pulse duration was 110 fs. In addition, the parabolic shape of the pulses should allow much higher B integral values when pulses are further amplified in the FCPA system.

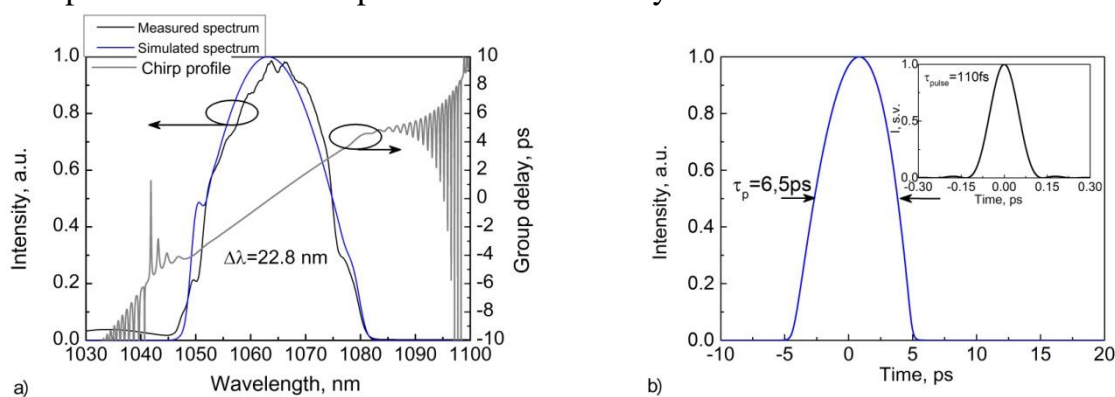**Fig.19. a)** Measured output spectrum on linear scale of the Yb-doped amplifier (black color) that is seeded by 380 fs oscillator pulses in comparison with simulated (blue color); simulated chirp profile of pulses at the output of fiber system (grey color); **b)** calculated envelope of the generated parabolic pulses; inset: calculated envelope of transform limit of generated parabolic pulses.

Chapter 4: Femtosecond fiber laser systems for seeding and pumping of the optical parametric amplifier

In this chapter a couple of fiber CPA systems, that use large diameter photonic crystal fibers, are presented. Besides, optimization of those systems is described.

Chapter 4.1: Fiber CPA system based on pulse amplification in the flexible 40 µm diameter photonic crystal fiber amplifier

A principal optical scheme of the fiber CPA system that uses the 40 µm diameter photonic crystal fiber for the pulse amplification is illustrated in Fig.20. For the sake of clarity three main parts of this system can be distinguished: a fiber seed source of the power amplifier, the power amplifier based on PCF and the pulse compressor. The seed source consisted of the passively mode-locked fiber oscillator, three preamplifiers, the stage of formation of spectral and temporal characteristics and the pulse picker. In this system chirped pulses were amplified in a commercially available photonic crystal fiber *aeroGAIN-FLEX* (*NKT Photonics*) with the 40 µm core diameter and the 1.8 m length. The amplified pulses were compressed using diffraction gratings of 1600 gr/mm.
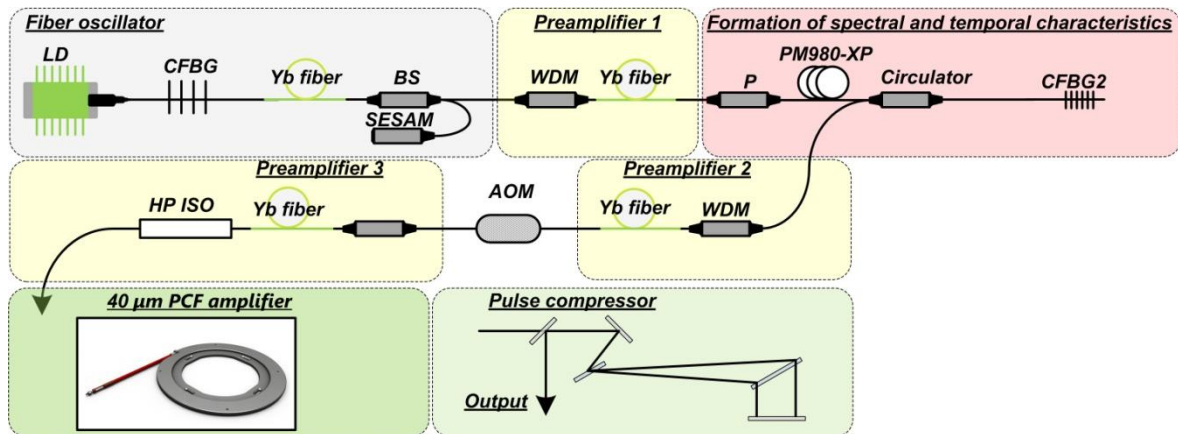

Fig. 20. A principal layout of the fiber CPA system using the 40 µm diameter photonic crystal fiber amplifier.

Firstly, the scheme and characteristics of the system seed source are discussed. The initial pulses of the system were generated in a passively mode-locked all-in-fiber oscillator, operating at the 1030 nm central wavelength. The initial pulses with the duration of 1 ps were generated at the 40MHz repetition rate in the linear cavity consisting of FBG, the 6 µm Yb doped fiber, the beam splitter and a saturable absorber mirror (SESAM). One of desired properties of the seed pulse for the fiber CPA system is that the spectrum of the seed pulses must be smooth, as any ripples in the spectrum will be transformed into the ripples of the temporal envelope when pulses are stretched [27].

These temporal ripples will be enhanced in the nonlinear fiber amplifier. In order to form a smooth shape of the pulse spectrum by reducing spectral modulations different techniques were employed. Firstly, CFBG with optimized the reflection profile was used in the fiber oscillator to reduce the intensity of Kelly sidebands (Fig. 21 inset). Secondly, in order to broaden the spectrum of the pulse and avoid the occurrence of modulation, a low pulse energy (0.58 nJ) and a long passive fiber (50 m) were used. The broadened spectrum and
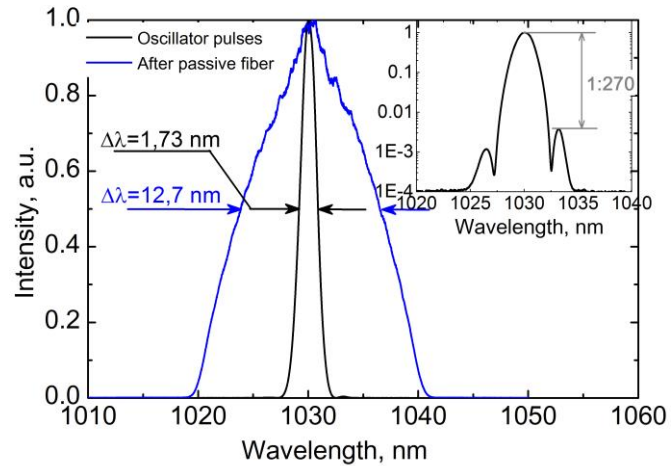

Fig.21. The broadened spectrum of oscillator pulses using 0.58 nJ energy and long (50 m) passive fiber (blue color) as well as spectrum of oscillator pulses (black color); inset: measured spectrum of oscillator pulses on logarithmic scale.

as well as the spectrum of the oscillator are shown in Fig. 21. The spectrum of the oscillator on a logarithmic scale is illustrated in the inset of Fig.21. and it shows the intensities of Kelly sidebands. Spectrally broadened pulses were directed to the CFBG stretcher of 40 ps/nm through the circulator and were stretched to the 500 ps duration. In order to achieve the required energy of seed pulses two preamplifiers were used. The pulse repetition rate was reduced using the acousto-optic modulator.

Chirped pulses were amplified using the photonic crystal fiber with the core diameter of 40 μm (mode field diameter - 31 μm, mode area - 760 μm^2). A principal scheme of the commercially available PCF amplifier (*aeroGAIN-FLEX, NKT Photonics*) is depicted in Fig.22. The polarization maintained double clad ytterbium doped fiber (DC-200/40-PZ-Yb) was used in this module. One of ends of the Yb fiber is spliced to the passive fiber with the diameter of 10 μm through the mode adapter at which a residual part of the pump is absorbed. This passive fiber of the amplifier module was spliced with the output fiber of the seed source, therefore all the fiber design of the system was realized. The output end of the amplifier module had the endcap and the pump radiation from the pigtailed laser diode was inserted through the output of the amplifier (Fig.22.).
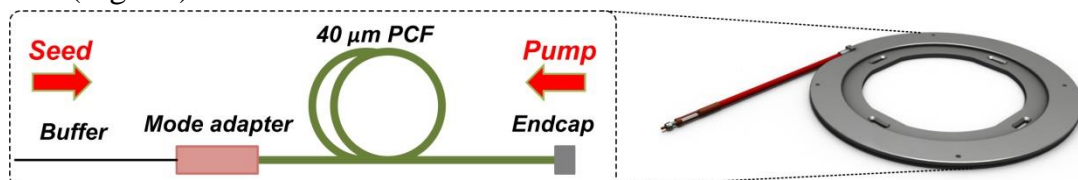

Fig. 22. A principal scheme of the amplifier module based on photonic crystal fiber.

Measured characteristic of amplification at the 40 MHz repetition rate are depicted in Fig.23. The efficiency of amplification was saturated at 60 % at 40 W of the

pump power while the average power of initial pulses was 385 mW. The variation of the output power at the 66 W pump power by changing the average power of the seed is depicted in the inset of Fig.23. Decreasing the average power of seed pulses 4 times the average power of the output decreases only by 3.4 %, which means that the amplifier can be saturated using small seed. Lowering of seed the output power decreases even more. The efficiency of amplification reached 50 % and the average power of the seed pulse
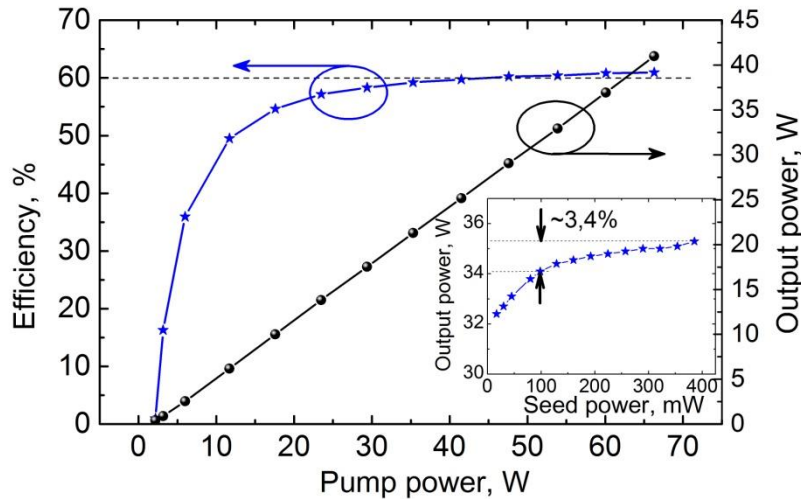

Fig.23. Measured dependences of output power (black colors) and efficiency (blue color) of the PCF amplifier on pump power at 40 MHz repetition rate; inset: output power of the PCF amplifier versus seed power at 66 W pump power.

was reduced to 17 mW. The reduction of the seed power/energy can be useful for reducing the value of a nonlinear phase accumulated in the amplifier. In order to demonstrate this principle, the experiment of amplification of pulses at the 1 MHz repetition rate was performed. The pulses with a different initial pulse energy were amplified up to the 20 μJ pulse energy (measured after the pulse compressor). Measured autocorrelation traces of compressed pulses as well as parameters of the pulse quality are depicted in Fig. 24a. These measurements show that the pulse quality of compressed pulses is better when the energy of initial pulses is reduced. This result can be explained
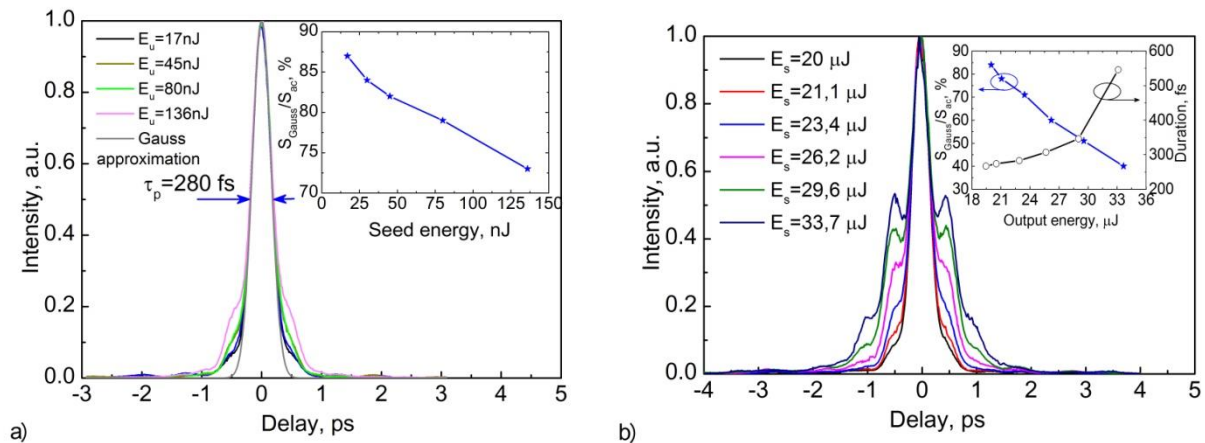

Fig. 24. a) Measured autocorrelation traces at 20 μJ output energy by varying seed energy; inset: dependences of pulse quality parameters and pulse duration on the output energy.

as follows: the maximum pulse energy at lower seed is achieved closer to the amplifier end and therefore the section of the Yb fiber acting as a passive fiber is shorter. Therefore, the reduction of seed enables improving the temporal quality of compressed pulses. However, increasing the output energy more, the impact of the amplifier nonlinearity increases. This can be seen from measured autocorrelation traces of compressed pulses amplified up to the different energy (Fig.24b). One of the most relevant issues is to determine how much energy with the satisfied pulse quality can be achieved. In this work the pulse quality is considered to be satisfactory when S_{Gauss}/S_{AC} is no less than 70%, therefore at this level the achieved pulse energy is 23.4 µJ and the pulse duration is 280 fs.

Chapter 4.2: Fiber CPA system based on pulse amplification in the rod type 55 µm diameter photonic crystal fiber amplifier

In the previously described fiber CPA system the impact of amplifier nonlinearities on the pulse quality was significant at the pulse energy above 20 µJ. In this work for reducing the accumulated nonlinear phase and achieving the higher pulse energy the 55 µm diameter PCF amplifier was used. A principal layout of the CPA system that uses the 55 µm core diameter PCF amplifier was similar to the previously discussed one (Fig. 20); it consisted of the fiber seed source, the power amplifier and the pulse compressor. However, the seed source for this CPA system had some differences caused by features of the PCF amplifier. A principal layout of the seeder is depicted in Fig. 25. The initial pulses with the duration of 1 ps were generated at the 45 MHz repetition rate in a passively mode-locked fiber oscillator operating at the 1030 nm
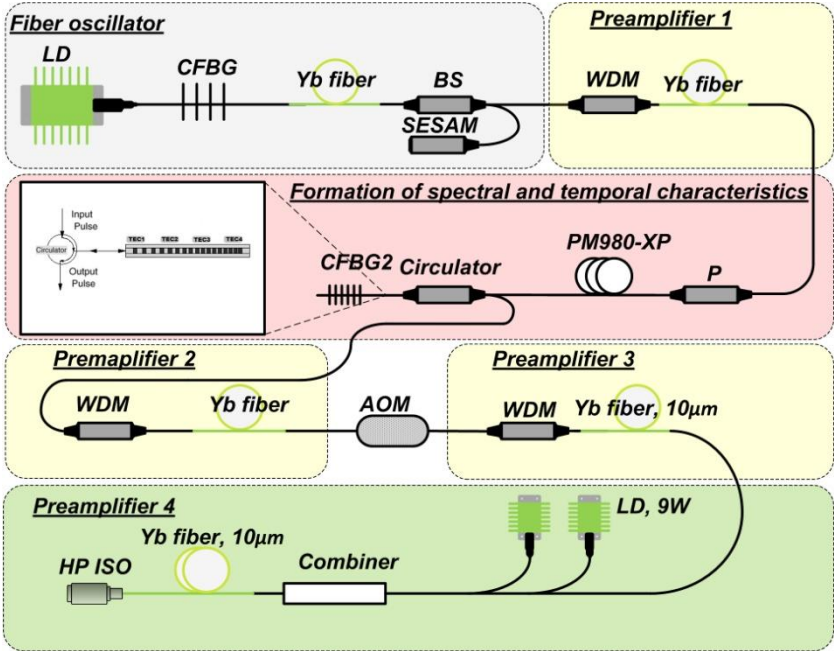

Fig.25. A principal layout of a fiber seed source for the rod type PCF amplifier.

central wavelength. Oscillator pulses were amplified up to the 0.51 nJ energy in the Yb doped single mode fiber amplifier and were spectrally broadened in the 50 m of passive fiber. The spectrum of pulses after the passive fiber as well as the spectrum of oscillator pulses were the same as shown in Fig. 21. Spectrally broadened pulses were stretched up to 500 ps using the CFBG stretcher with dispersion of 40 ps/nm. After that chirped pulses were amplified in two stages of preamplifiers. The pulse repetition rate in this system was changed by use of the acousto-optic modulator. Contrary to the previous CPA system the last preamplifier of the seed source had a double clad Yb doped fiber with the diameter of 10 μm pumped by a couple of multimode laser diodes. This concept of the last preamplifier enabled us to achieve the ~1 μJ level pulse energy at the 1 MHz repetition rate that is necessary for this PCF amplifier.

In this fiber CPA system chirped pulses were amplified in a commercially available photonic crystal fiber *aeroGAIN-ROD* (*NKT Photonics*) with the core diameter of 55 μm (mode field diameter - 45 μm, mode area - 1600 μm^2) and the length of 0.8 m. Both the seed pulse and the pump radiation were introduced in the amplifier module through a free space, therefore this CPA system is less compact than the previously described one. However, a larger core of the PCF amplifier enables one to achieve the higher pulse energy. Measured characteristics of amplification at 45 MHz repetition rate are depicted in Fig.26a. The efficiency of amplification was saturated at 48.5 % at 40 W of the pump power, while the average power of initial pulses was 1 W. The variation of the output power at the 60 W pump power by changing the average power of the seed power is depicted in Fig.26b. By reducing the average power of seed pulses 4 times (up to 250 mW) the average power of the output decreases to 18.9 W (~22 %), which means that the efficiency of amplification strongly depends on the seed power. Including losses of optics the efficiency of 53 % was obtained at the 2 W seed power. The dependence
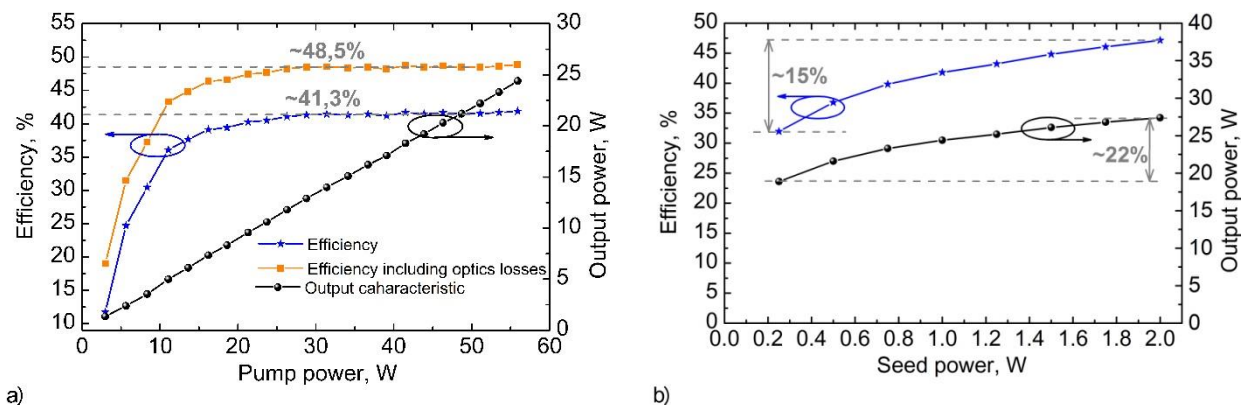
Fig. 26. Measured output power (black color) and efficiency (blue and orange colors) of the PCF ROD amplifier versus pump power **(a)** and seed power **(b)** at 45 MHz repetition rate.

of the output power on the seed power revealed that the efficiency of amplification grew increasing the seed power. However, in order to achieve the highest pulse energy with a good temporal pulse quality at the system output it is necessary to find out the optimal seed power. Fig.27a shows the achievable pulse energy at the 60 W pump power by

amplifying seed pulses of the 0.7 μJ, 1 μJ and 1.2 μJ energy. Despite that the pulse energy at the system output differs only by ~10 %, the temporal quality of compressed pulses differs considerably. This can be clearly seen from variation of the pulse quality parameters (S_{Gauss}/S_{AC}) at a different seed energy shown in Fig.27b. Reducing the seed energy from 1.4 μJ to 0.7 μJ the achieved pulse energy at the S_{Gauss}/S_{AC} ~70 % level (that shows a satisfied pulse contrast) increased from 38 μJ to 52 μJ. The measured autocorrelation trace of compressed 52 μJ energy pulses is depicted in Fig.28. The duration of 280 fs was obtained.
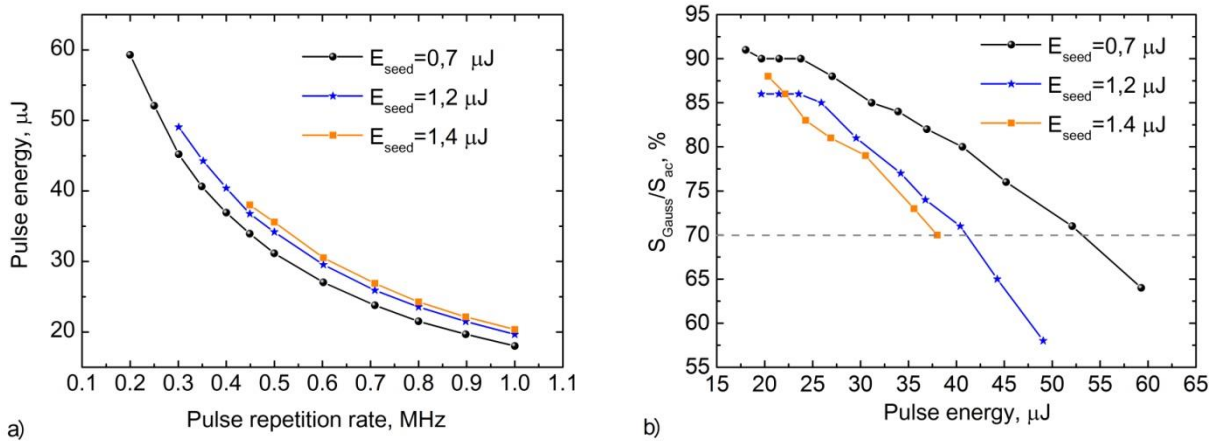

Fig.27. a) Measured pulse energy at the output of system at different pulse energy of initial pulses; b) a dependence of temporal quality of compressed pulses on pulse energy at different pulse energy of initial pulses.
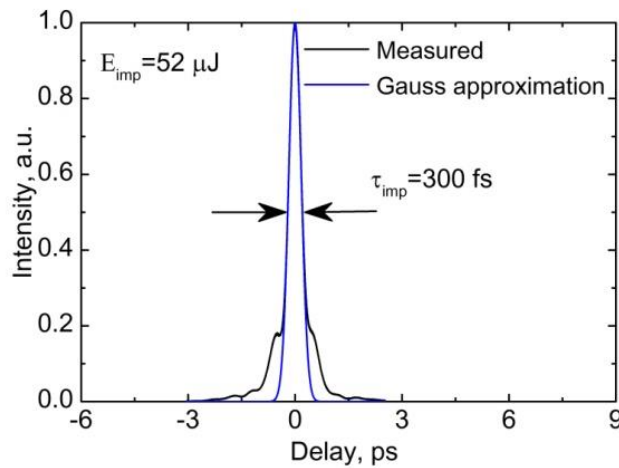

Fig.28. Measured autocorrelation trace of compressed pulses at 52 μJ pulse energy.

Chapter 5: Frequency conversion of the ultrafast fiber laser using the optical parametric amplifier

In this chapter the experiments of the continuum generation in a bulk material with pump pulses from the fiber femtosecond laser operating at the 1 MHz repetition rate are presented. Moreover, the efficient operation of a tunable femtosecond optical parametric amplifier (OPA) based on the BiBO pumped at 515 nm by the 1 MHz fiber laser is presented. Finally, this work is summarized by presenting a tunable femtosecond laser system based on the optical parametric amplifier pumped by the femtosecond fiber laser.

Chapter 5.1: Continuum generation in the bulk materials by high repetition rate pulses

The initial task of developing the laser system based on the OPA is to form seed pulses of a broad spectrum. In this work a continuum (white-light) generated by the femtosecond fiber laser operating at the 1030 nm wavelength was chosen. However, contrary to other works in this study the continuum radiation in bulk materials was generated using a high, 1 MHz repetition rate. Therefore, one of the tasks of this study was to determine the pump energy threshold, optimal focusing conditions in several bulk crystals and the optimal material for the continuum generation by pump pulses from the fiber femtosecond laser operating at the 1 MHz repetition rate.

Single crystals of the 5 mm thick yttrium aluminum garnet (YAG), 4 mm thick yttrium vanadate (YVO$_4$) and the 6 mm thick sapphire plate were obtained commercially and used in this work. These materials are common laser host crystals and were chosen because of their high damage threshold and a good crystalline quality. All crystals except YAG with its cubic crystalline structure were cut oriented along the optical axis to avoid birefringence. They were undoped, without coatings and were used at room temperature. The setup of the continuum generation in crystals is depicted in Fig. 29. In all of experiments reported in this study the continuum generation was
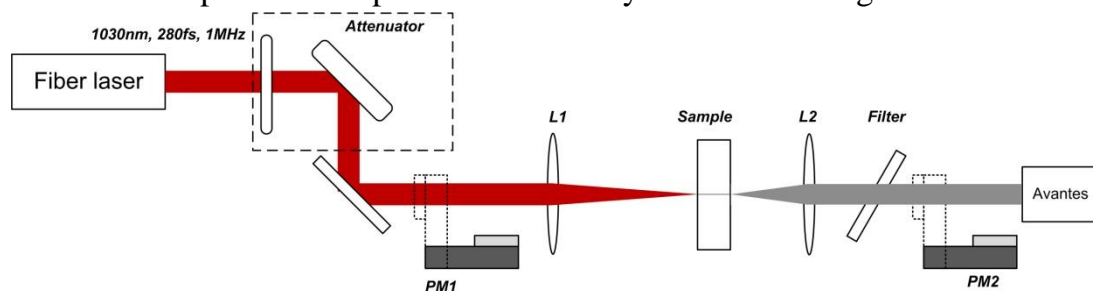

Fig.29. A layout of experimental setup of continuum generation in bulk crystals.

initiated by pulses from a fiber laser (described in chapter 4.1), which delivered pulses of the 280 fs duration at a center wavelength of 1030 nm with the repetition rate of 1 MHz in a collimated beam with the diameter of 5 mm. The pulse energy was adjusted using a variable density attenuator. Pulses were focused with a lens (L1) into the respective crystal to start the continuum generation and the generated continuum was collimated with the 25 mm lens (L2). A grating-based spectrograph with a silicon CCD detector (*Avantes*) was used to record the spectrum of the continuum. Typical spectra of the continuum generated in the sapphire plate using a +50 mm focusing length (numerical aperture (NA) 0.02) are shown in Fig.30a. Exceeding the pump energy threshold (1.3 µJ) the spectrum of initial pulses suddenly spreads out and increasing the pump energy intensity of the continuum the spectrum increases. The intensity of the continuum
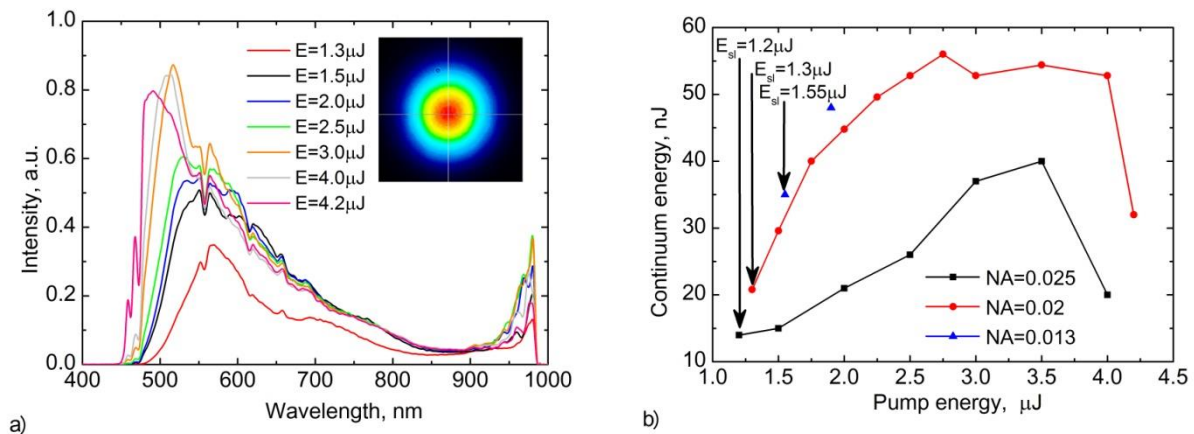

Fig.30. a) A typical variation of continuum spectra increasing energy of pump pulses in a sapphire plate; inset – beam profile of generated continuum **b)** a dependence of continuum energy on pump energy at different NA.

spectrum was saturated at ~3 µJ and the sapphire plate was damaged optically at the pulse energy of 4.2 µJ. A variation of continuum spectra under different focusing conditions was very similar and the dependence of the continuum energy on pump energy at various NA is depicted in Fig.30b. Vertical arrows in Fig.30b label the pump energy thresholds. A life-time of the generated continuum was also measured under different NA. Long-term measurements of the continuum energy were performed by choosing the same level of the pump energy (~20 % above the generation threshold) (Fig.30b). The continuum was generated for 90 hours without a noticeable damage of the crystal at NA=0.02, when the continuum became unstable after 30 hours operation and the energy of the continuum dropped significantly in the first hour at NA=0.025 and at NA=0.013, respectively.

For the continuum generation in the YAG crystal lenses with a +40 mm and +50 mm focal length were used. Measured continuum thresholds were 480 nJ and 630 nJ, respectively. The dependence of the continuum spectrum on the pump energy is depicted in Fig.32a. Increasing the pump energy above the generation threshold a small spectral broadening was observed. Contrary to the generation in the sapphire crystal in this case the window of the continuum generation was very narrow - at 10-15 % above
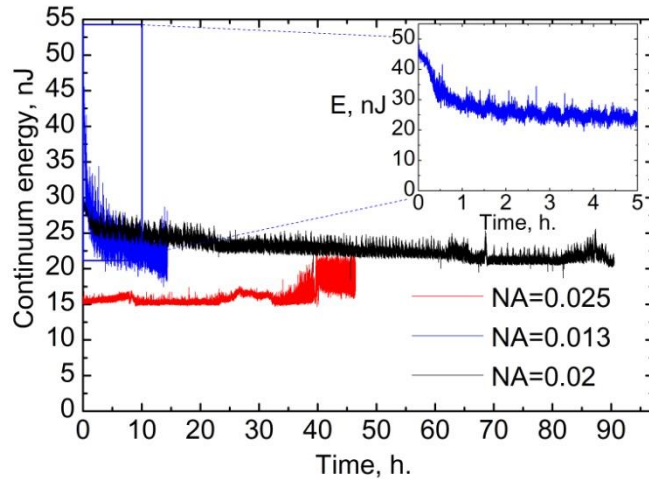
Fig.31. Measured long term stability of the continuum energy in a sapphire plate at different focusing conditions.

the threshold the continuum spectrum became narrow and the energy of continuum was decreased significantly. A continuous continuum generation in the energy range of 0.5-1.2 µJ was obtained by adjusting the position of the crystal in relation to the focus. Due to this fact a threshold of the continuum generation increased to 520 nJ (NA=0.025). A long-term measurement of the continuum energy using this crystal position at the 600 nJ pump pulse energy was performed- a continuous operation of the continuum for 70 hours without the crystal damage was observed. The measured threshold of the continuum generation in the YVO4 crystal was two times lower than in the YAG crystal. Measured thresholds of the continuum thresholds were 230 nJ and 270 nJ (using lenses with a +40 mm and +50 mm focal length, respectively).
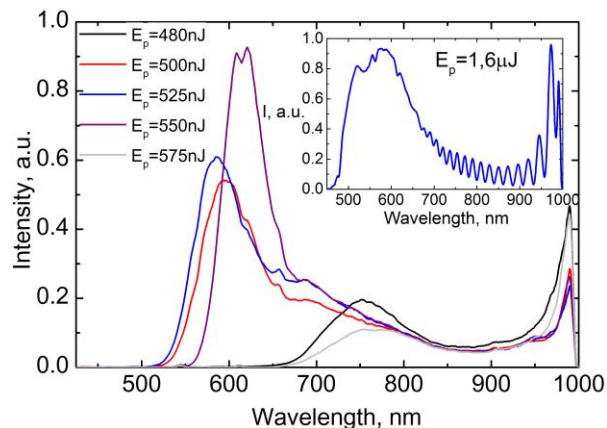
Fig.32. A typical variation of continuum spectra increasing the energy of pump pulses in YAG crystal; inset - continuum spectrum in the second filament generation regime.

Chapter 5.2: Research of continuum amplification

In this work beta barium borate (β-BaB$_2$O$_4$, BBO) and bismuth triborate (BiB$_3$O$_6$, BiBO) nonlinear crystals for the optical parametric amplification of the continuum were chosen. BiBO is a birefringent nonlinear crystal, also belonging to

the borate family of materials, possesses unique linear and nonlinear optical properties for the frequency conversion. Firstly, BiBO offers versatile phase-matching properties and flexible wavelength-tuning characteristics, with an effective nonlinear coefficient as high as 3.7 pm/V [28], which is nearly twice and four times larger than those of BBO and LBO crystals, respectively. Secondly, as a biaxial crystal, BIBO also offers a large angular and spectral acceptance bandwidth, low spatial walk-off, and a broadband angle tuning at room temperature. Thirdly, it is also non-hygroscopic and is readily available of the high optical quality, a large size, and at low cost. Owing to these features in this study the BiBO crystal has been chosen for the continuum amplification.
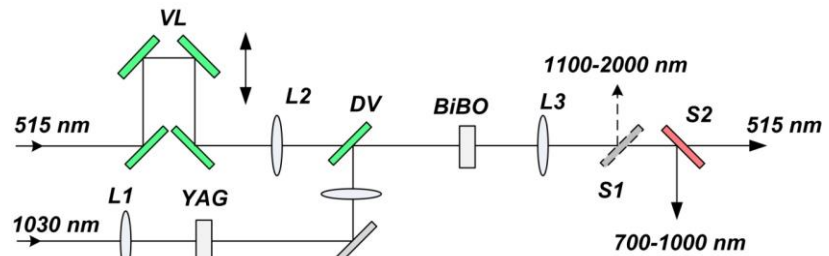

Fig.33. A principal layout of collinear OPA seeded by a continuum generated in the YAG crystal.

In this work the continuum radiation was amplified using the OPA which was set up in a collinear geometry. The experimental setup of the continuum amplification is depicted in Fig.33. The seed source of the OPA was a continuum generated in the 5 mm YAG crystal by pump pulses from the fiber laser operating at the 1030 nm wavelength and generating pulses of the 280 fs duration at the 1 MHz repetition rate. The second harmonic of 515 nm has been generated and used to pump the OPA. The pump and seed beams were combined with a broad- band dichroic mirror (DM), which had a high transmission at the 515 nm wavelength. The focal diameters of the seed and pump beams at the nonlinear crystal were of the order of 60 μm. The temporal overlap was adjusted by a variable delay line (VDL). For optical parametric amplification the 2 mm thick BBO ($\theta=23.4^0$, $\varphi=0^0$), 1 mm and 2 mm thick BiBO ($\theta=171^0$, $\varphi=90^0$) crystals were used. Both of the crystals were cut for type I phase matching. Recollimation was done with an achromatic lens (L3). Signal and idler waves were separated using separators S1 and S2. The wavelength tuning was performed by simply changing the phase-matching angle and readjusting the variable-delay line. Dependences of the energy of signal waves and the efficiency on the pump energy using BBO and BiBO nonlinear crystals are depicted in Fig.34. Saturation of the signal energy using the BBO crystal for amplification has been achieved at the 1 μJ pump energy. The efficiency of conversion from the pump to the signal of 10-12 % depending on the spectral range was obtained. Meanwhile the signal energy was saturated at the 2.5 times lower pump energy using the 2 mm thick BiBO crystal. The efficiency of 10-12 % depending on the spectral range was obtained at the 0.4 μJ pump energy. The main result of this experiment is that the effective amplification of the continuum in the BiBO crystal was achieved at a low pump energy. This result can be attributed to the larger nonlinear refractive index of the BiBO crystal. The experiments of the continuum
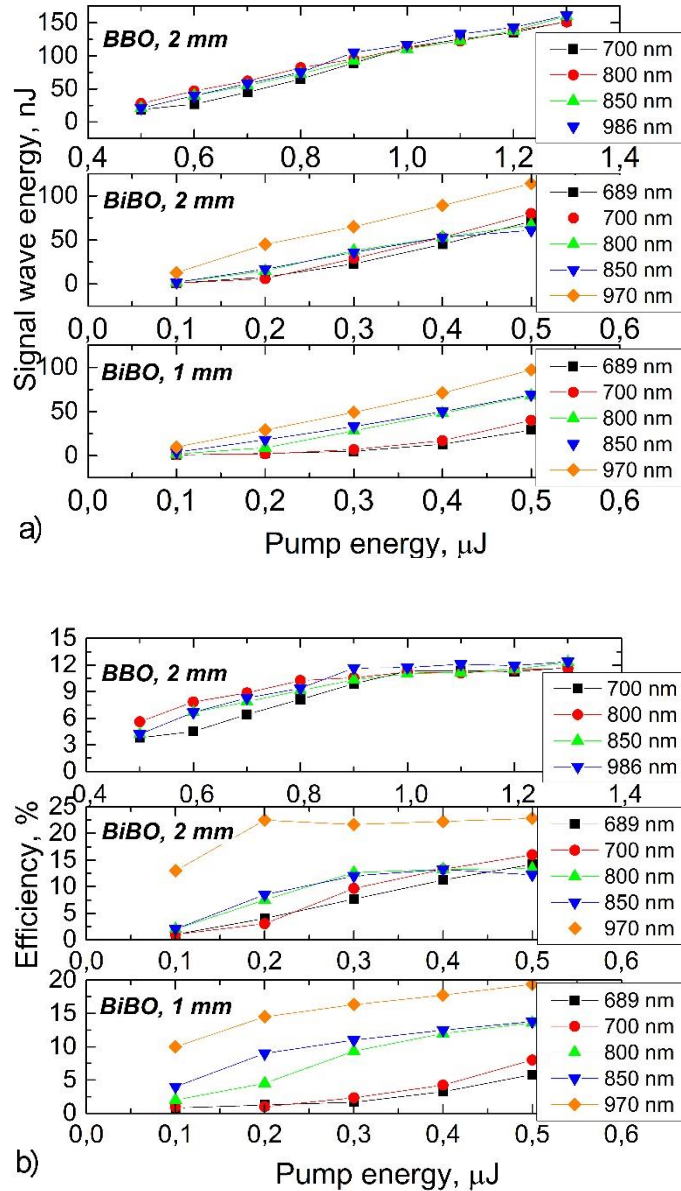
Fig.34. Dependences of amplified signal energy (a) and amplification efficiency (b) on pump energy using BBO and BiBO crystals.

amplification by varying diameters of seed and pump beams were also presented in this chapter. An effective amplification was obtained using beams with the diameter of 60 μm at a low pump energy, however, the beam of the signal wave had astigmatism. The spatial quality of the beam was improved by increasing diameters of seed and pump beams up to 115 μm. The enlargement of beam diameters requires the higher pump energy in order to achieve the same conversion efficiency. In case of the BiBO crystal the efficiency of 10-12 % was obtained at the 1uJ pump energy, while beam diameters were 115 μm. In case of the BBO crystal under the same conditions the required pump energy should be significantly higher, about ~3 μJ. Because of this feature a BiBO crystal is a very attractive candidate for the frequency conversion applications in compact tunable laser systems.

Chapter 5.3: Tunable femtosecond laser system based on OPA pumped by the femtosecond fiber laser

In this chapter the tunable femtosecond laser system based on the OPA pumped by the femtosecond fiber laser is presented. A principle layout of the system is sketched in Fig.35. The system consisted of five main parts: first, a femtosecond fiber μJ/MHz pump laser; second, a continuum generation stage; third, a frequency doubling stage; fourth, an OPA stage; and finally, a pulse compression setup based on a pair of prisms. The seed and pump pulses of the OPA were generated by the fiber laser (described in detail in chapter4.1) operating at the 1030 nm wavelength and generating pulses of the 280 fs duration at the 1 MHz repetition rate with the energy of up to 20 μJ.
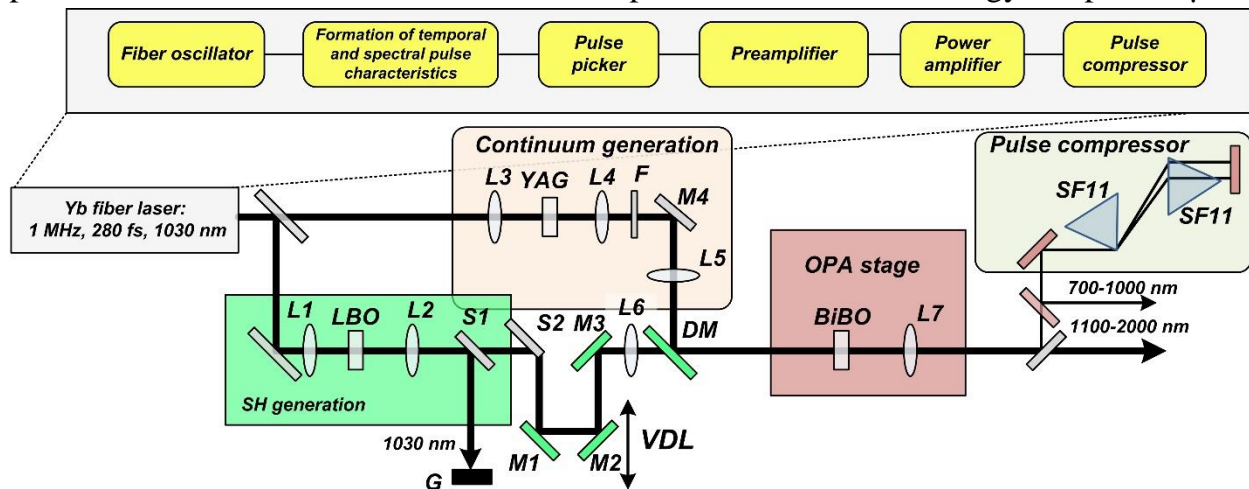
Fig.35. A principle layout of a tunable femtosecond laser system based on OPA pumped by femtosecond fiber laser.

For the present experiment the output of the laser was attenuated and the remaining part of the energy was divided into two parts. One part of the energy was used to generate a broadband signal (continuum) for seeding OPA, another part of the energy was used for the frequency doubling. The pump of OPA was a second harmonic (SH) of the fiber laser generated in a 3.7 mm thick lithium borate (LBO) crystal under critical type I phase-matching conditions ($\theta=90^0$, $\varphi=13.8^0$). The spot size at the LBO crystal was approximately 200 μm, leading to the efficiency of frequency doubling of nearly 65 %. After the frequency doubling the SH was collimated by the lens (L2) and separated from the infrared fraction by separators S1 and S2. Another part of the laser energy (600 nJ) was focused by the lens (L3, f=+40 mm, NA=0.025) onto a 5-mm thick YAG crystal to generate a white light continuum. A broadband radiation was collimated by the achromatic lens (L4), filtered (F) and directed to an OPA stage. The pump and seed beams were combined with a broadband dichroic mirror (DM), which had a high transmission at the 515 nm wavelength. The focal diameters of the seed and pump beams at the nonlinear crystal were of the order of 115 μm. The temporal overlap was adjusted by a variable delay line (VDL). For the optical parametric amplification a 2 mm thick BiBO crystal (($\theta=171^0$, $\varphi=90^0$)) was used. The wavelength tuning was performed by
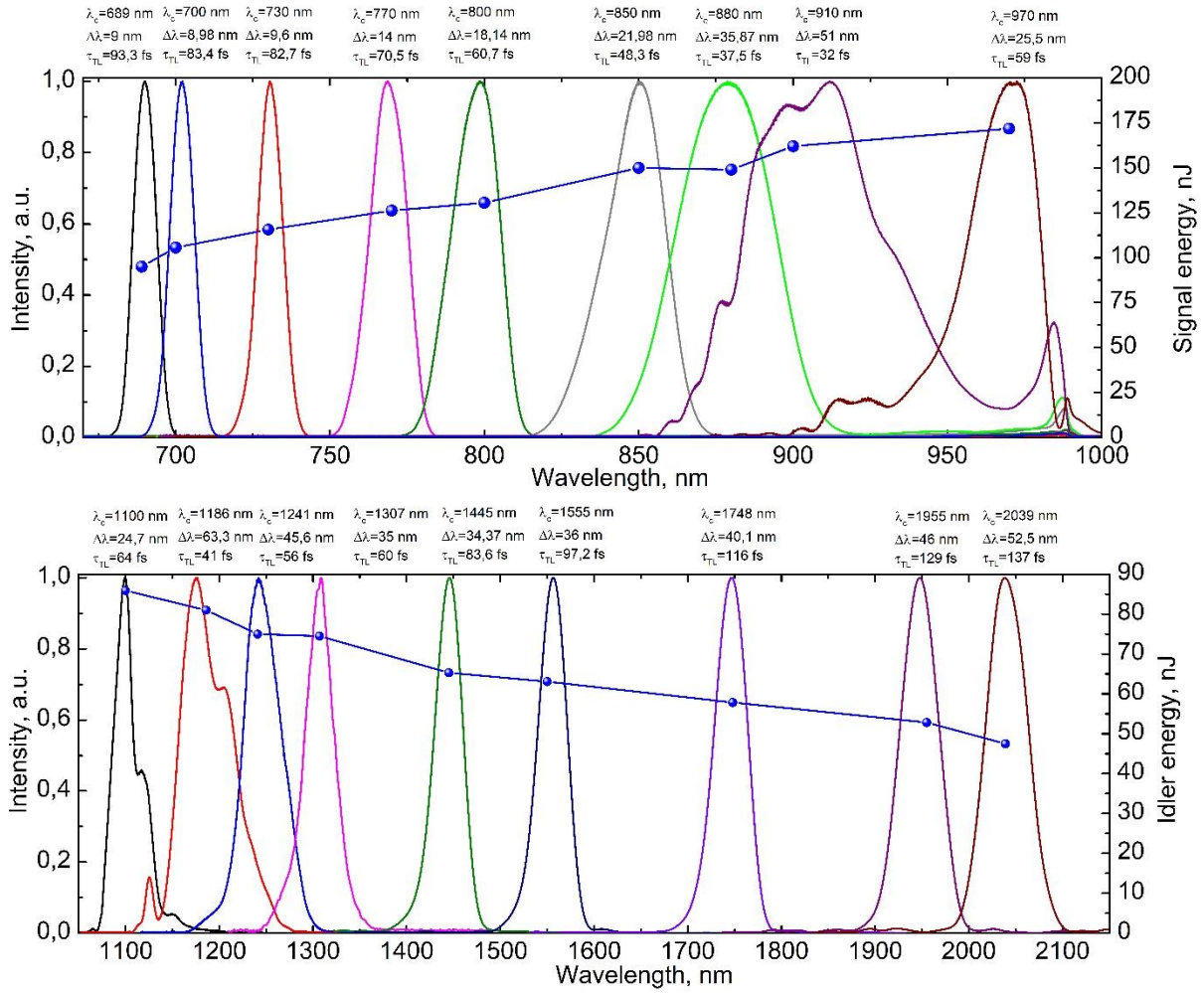
Fig.36. Measured pulse spectra and pulse energy at the system output when performing wavelength tuning.

simply changing the phase-matching angle and readjusting the variable-delay line. The pulses were characterized by use of optical spectrum analyzers *YOKOGAWA AQ6370D* (for signal) and *YOKOGAWA AQ6375B* (for idler). Measured output spectra from the system at a different central wavelength are shown in Fig.36. The tuning range of output pulses was 690-970 nm and 1100-2050 nm and it was limited by the amplification bandwidth of the BiBO crystal. Above each measured spectrum values of the bandwidth and the corresponding duration of transform limited pulses are presented. Besides, the output energy of the signal and the idler at the pump pulse energy of 1 µJ is shown in Fig.36. The efficiency of conversion from the pump to the signal of 9.5-17 % at the 1 µJ pump energy depending on the spectral range was obtained.

The signal and the idler after the OPA stage were separated by dichroic mirrors and signal pulses were directed to a pulse compressor. The pulses were compressed using a pair of Brewster angle prisms made of SF11 glass. For the characterization of compressed pulses a multiple-shot SHG FROG autocorrelator was used. Retrieval calculations of the pulse envelope using the FROG algorithm (*Swamp Optics*) for the measurements at 730 nm and 850 nm central wavelengths were performed (Fig.37.) The pulse durations calculated from measured autocorrelation traces

and FROG retrievals were similar and equal to 83.6 fs and 52 fs, respectively. The obtained pulse durations for other wavelengths are presented below in Table 1.

a)   b)

Fig.37. Envelopes of compressed pulses retrieved using the FROG algorithm for the measurements at 730 nm (a) and 850 nm central wavelengths (b).

Table 1. The duration of compressed pulses as well as duration of tranform-limited pulses and bandwidth of the signal spectrum.

λ_c, nm	τ_p, fs	τ_{TL}, fs	$\Delta\lambda$, nm
730	83,6	82,7	9,6
770	72	70,5	14
800	62	60,7	18,14
850	52	48,3	21,98
880	39,2	37,5	35,87
910	47	32	51

Measurements of the idler generated at the OPA stage using the same multiple-shot SHG FROG autocorrelator were performed. Retrieval calculations of the pulse envelope using the FROG algorithm for the measurements at 1450 nm and 1550 nm central wavelengths were performed (Fig.38.) The pulse durations calculated from measured autocorrelation traces were similar to FROG retrievals and equal to 133 fs and 117 fs, respectively. In

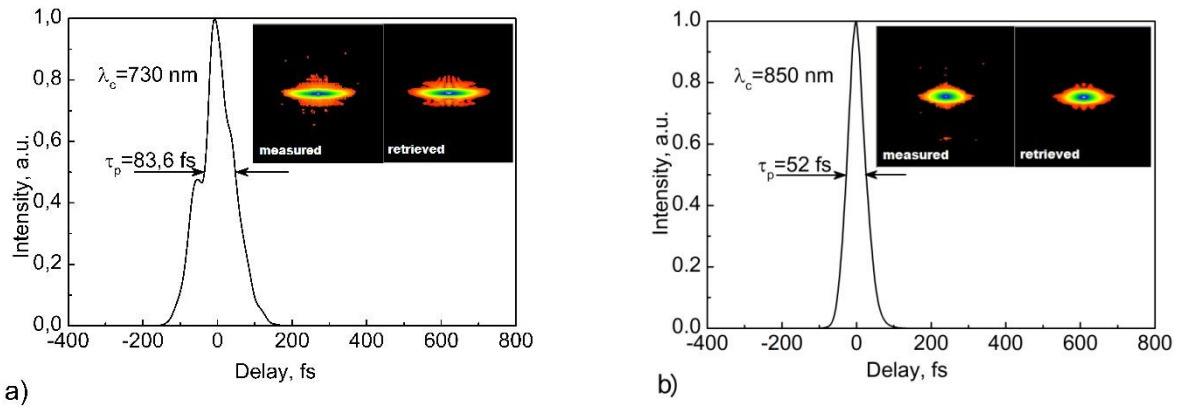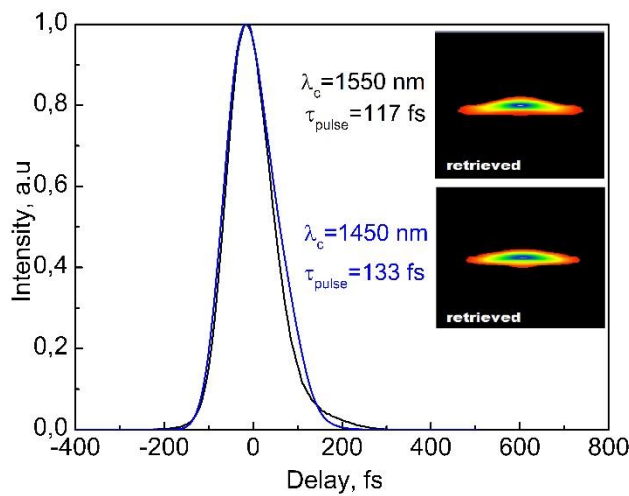**Fig.38.** Envelopes of idler pulses retrieved using the FROG algorithm for the measurements at 1550 nm and 1450 nm central wavelengths.

order to characterize the beam quality at the output of the system, the dependence of the beam radius on the distance from the focal plane was measured at different wavelengths of the signal pulse. M^2 factor was calculated to be <1.3 in the spectral range of 690-880 nm and <1.5 for 970 nm wavelength.

Main results and conclusions

1. All-in-fiber passively mode-locked fiber oscillators that use chirped fiber Bragg gratings of low dispersion for compensation of the normal cavity dispersion were implemented experimentally. The use of the low dispersion CFBG (0.25–0.82 ps/nm) allowed us to generate ultrashort pulses with the duration of 0.38-1.2 ps. Besides, the impact of CFBG characteristics on oscillator pulses was investigated. It has been shown that optimizing the bandwidth of the CFBG the reflection, intensity of Kelly sidebands - typical of soliton pulses – can be reduced significantly without the pulse lengthening. Also, it has been shown that linearly chirped parabolic pulses with the bandwidth of 22.8 nm and the duration of 6.5 ps can be generated in the ytterbium doped fiber amplifier by fiber soliton mode-locked oscillator, which generates pulses with the duration of 380 fs at the 1064 nm central wavelength.

2. In the fiber CPA system in which stretched pulses with the duration of 300 ps were compressed by the diffraction grating (1600 gr/mm), the TOD introduced by the pulse compressor can be compensated by optimizing the chirp profile of CBFG stretcher. This compensation enables one to achieve high fidelity pulses with the duration of few hundreds fs at the output of the system. A numerical simulation of fiber CPA system in which the initial pulses of different duration were stretched up to duration of 350 ps and stretched spectrally up to 7.5 nm and were compressed by the diffraction grating (1600 gr/mm) was performed. It was found that the temporal quality of compressed pulses at the output of this fiber CPA system can be improved using the initial pulses with shorter duration due to smaller accumulated nonlinear phase.

3. In this work a novel fiber CPA system consisting of the tunable dispersion CFBG stretcher and the fixed dispersion CVBG as a pulse compressor was presented. It was found that a distortion of linear chirp profile of pulse stretcher/compressor limits the temporal quality of compressed pulses that can be improved only by matching dispersion profiles of CFBG stretcher and CVBG compressor.

4. By combining various fiber technologies described in this study fiber CPA systems were investigated. Stretched pulses with the duration of 500 ps were amplified in photonic crystal fiber amplifiers with the core diameter of 40 μm and 55 μm up to the 20-50 μJ pulse energy. High fidelity pulses with the duration less than 300 fs were achieved at the output of systems. These pulses can be used to pump the optical parametric amplifier operating 1 MHz repetition rate.

5. In this work the research of continuum amplification in BBO and BiBO nonlinear crystals was performed. It was found that amplification efficiency of 10-12 % in BiBO crystal is achieved at 2.5 times lower pump energy compared with BBO crystal. Therefore, the BiBO crystal is more preferable realizing wavelength tunable fiber laser systems with pulse energy of the order of 1 μJ. It was

experimentally demonstrated that the continuum generation in the 5 mm thick YAG crystal and continuum amplification in the 2 mm thick BiBO crystal enables us to realize a femtosecond laser system with wavelength tuning in the range of 690 nm-2040 nm and operating at the 1 MHz repetition rate.

Bibliography

1. G. Cerullo and S. De Silvestri, "Ultrafast optical parametric amplifiers," Rev. Sci. Instrum. **74**, 1–18 (2003).
2. M. Nisoli, S. De Silvestri, V. Magni, O. Svelto, R. Danielius, and A. Piskarskas, "Highly efficient parametric conversion of femtosecond Ti:sapphire laser pulses at 1 kHz.," Opt. Lett. **19**, 1973–1975 (1994).
3. V. V Yakovlev, B. Kohler, and K. R. Wilson, "Broadly tunable 30-fs pulses produced by optical parametric amplification," Opt. Lett. **19**, 2000–2002 (1994).
4. T. Wilhelm, J. Piel, and E. Riedle, "Sub-20-fs pulses tunable across the visible from a blue-pumped single-pass noncollinear parametric converter," Opt. Lett. **22**, 1494–1496 (1997).
5. A. Baltuška, T. Fuji, and T. Kobayashi, "Visible pulse compression to 4 fs by optical parametric amplification and programmable dispersion control," Opt. Lett. **27**, 306–308 (2002).
6. M. Ghotbi, M. Ebrahim-Zadeh, V. Petrov, P. Tzankov, and F. Noack, "Efficient 1 kHz femtosecond optical parametric amplification in BiB3O6 pumped at 800 nm," Opt. Express **14**, 10621–10626 (2006).
7. B. R. Masters, P. T. C. So, C. Buehler, N. Barry, J. D. Sutin, W. W. Mantulin, and E. Gratton, "Mitigating thermal mechanical damage potential during two-photon dermal imaging," J. Biomed. Opt. **9**, 1265–1270 (2004).
8. P. G. Antal and R. Szipocs, "Tunable, low-repetition-rate, cost-efficient femtosecond Ti:sapphire laser for nonlinear microscopy," Appl. Phys. B Lasers Opt. **107**, 17–22 (2012).
9. K. Wang, T.-M. Liu, J. Wu, N. G. Horton, C. P. Lin, and C. Xu, "Three-color femtosecond source for simultaneous excitation of three fluorescent proteins in two-photon fluorescence microscopy," Biomed. Opt. Express **3**, 1972–1977 (2012).
10. S. H. Cho, B. E. Bouma, E. P. Ippen, and J. G. Fujimoto, "Low-repetition-rate high-peak-power Kerr-lens mode-locked TiAl2O3 laser with a multiple-pass cavity," Opt. Lett. **24**, 417–419 (1999).
11. Á. Krolopp, A. Csákányi, D. Haluszka, D. Csáti, L. Vass, and A. Kolonics, "Handheld nonlinear microscope system comprising a 2 MHz repetition rate, mode-locked Yb-fiber laser for in vivo biomedical imaging," Biomed. Opt. Express **7**, 3531–3542 (2016).
12. S. Tang, J. Liu, T. B. Krasieva, Z. Chen, and B. J. Tromberg, "Developing compact multiphoton systems using femtosecond fiber lasers," J. Biomed. Opt. **14**, 30508 (2009).
13. J. Limpert, F. Roser, S. Klingebiel, T. Schreiber, C. Wirth, and T. Peschel, "The Rising Power of Fiber Lasers and Amplifiers," IEEE J. Sel. Top. Quantum Electron. **13**, 537–545 (2007).
14. M. N. Zervas and C. A. Codemard, "High Power Fiber Lasers: A Review," IEEE J. Sel. Top. Quantum Electron. **20**, 219–241 (2014).
15. C. Jauregui, J. Limpert, and A. Tünnermann, "High-power fibre lasers," Nat. Photonics **7**, 861–867 (2013).
16. T. Eidam, J. Rothhardt, F. Stutzki, J. Limpert, and A. Tünnermann, "Fiber

chirped-pulse amplification system emitting 3.8 GW peak power," Opt. Express **19**, 255–260 (2011).

17. A. Klenke, S. Hädrich, T. Eidam, and J. Rothhardt, "22 GW peak-power fiber chirped-pulse- amplification system," Opt. Lett. **39**, 6875–6878 (2014).

18. R. L. Fork, B. I. Greene, and C. V. Shank, "Generation of optical pulses shorter than 0.1 psec by colliding pulse mode locking," Appl. Phys. Lett. **38**, 671–672 (1981).

19. M. Baumgartl, B. Ortaç, J. Limpert, and A. Tünnermann, "Impact of dispersion on pulse dynamics in chirped-pulse fiber lasers," Appl. Phys. B Lasers Opt. **107**, 263–274 (2012).

20. S. M. J. Kelly, "Characteristic sideband instability of periodically amplified average soliton," **28**, 806–808 (1992).

21. G. P. Agrawal and H. A. Haus, *Applications of Nonlinear Fiber Optics* (Academic, 2002).

22. T. Bartulevičius, S. Frankinas, A. Michailovas, R. Vasilyeu, V. Smirnov, F. Trepanier, and N. Rusteika, "Compact fiber CPA system based on a CFBG stretcher and CVBG compressor with matched dispersion profile," **25**, 22806–22812 (2017).

23. K. Michailovas, A. Baltuska, A. Pugzlys, V. Smilgevicius, A. Michailovas, A. Zaukevicius, R. Danilevicius, S. Frankinas, and N. Rusteika, "Combined Yb/Nd driver for optical parametric chirped pulse amplifiers," Opt. Express **24**, 22261 (2016).

24. V. I. Kruglov, A. C. Peacock, J. D. Harvey, and J. M. Dudley, "Self-similar propagation of parabolic pulses in normal-dispersion fiber amplifiers," **19**, 461–469 (2002).

25. D. N. Schimpf, J. Limpert, and A. Tünnermann, "Controlling the influence of SPM in fiber-based chirped-pulse amplification systems by using an actively shaped parabolic spectrum.," Opt. Express **15**, 16945–16953 (2007).

26. P. L. Kelley, I. P. Kaminow, and G. G. P. Agrawal, *Nonlinear Fiber Optics* (Academic, 2001).

27. D. N. Schimpf, E. Seise, J. Limpert, and A. Tünnermann, "The impact of spectral modulations on the contrast of pulses of nonlinear chirped-pulse amplification systems.," Opt. Express **16**, 10664–10674 (2008).

28. M. Ghotbi and M. Ebrahim-Zadeh, "990 mW average power, 52% efficient, high-repetition-rate picosecond-pulse generation in the blue with BiB_3O_6," Opt. Lett. **30**, 3395–3402 (2005).

Santrauka

Šioje disertacijoje buvo tiriamas ultratrumpųjų impulsų spektrinių ir laikinių charakteristikų valdymas skaiduliniuose solitoniniu režimu veikiančiuose sinchronizuotų modų osciliatoriuose ir skaidulinėse čirpuotų (faziškai moduliuotų) impulsų stiprinimo sistemose. Taip pat šiame darbe aprašyti čirpuotų impulsų stiprinimo didelio šerdies skersmens (40 µm ir 55 µm) fotoninių kristalų skaidulose eksperimentai. Visa tai buvo reikalinga siekiant realizuoti skaidulines lazerines sistemas, kurių impulsų laikinės, energinės ir spektrinės charakteristikos yra tinkamos optinių parametrinių stiprintuvų, veikiančių ~1 MHz impulsų pasikartojimo dažniu, kaupinimui. Taip pat buvo sukurta ir šioje disertacijoje aprašyta lazerinė sistema, generuojanti <150 fs trukmės impulsus spektro ruože nuo 700 nm iki 2040 nm.

Šiame darbe buvo tiriami skaiduliniai solitoniniu režimu veikiantys sinchronizuotų modų osciliatoriai, kuriuose normalios rezonatoriaus dispersijos kompensavimui buvo panaudotos mažos dispersijos (0,25-0,82 ps/nm) skaidulinės čirpuotos Brego gardelės. Tokie skaiduliniai osciliatoriai generavo trumpesnius nei 1,2 ps trukmės impulsus dešimčių MHz impulsų pasikartojimo dažniu ir yra patrauklūs kaip skaidulinių čirpuotų impulsų stiprinimo sistemų užkrato šaltiniai. Taip pat buvo pademonstruota, jog tiesiškai čirpuotų parabolinės formos impulsų generacija skaiduliniame stiprintuve galima santykinai ilgais, 380 fs trukmės, impulsais, generuojamais skaidulinio sinchronizuotų modų osciliatoriaus. Šis metodas leidžia suformuoti impulsus, turinčius tiesinį čirpą, kurį kompensavus būtų generuojami ~110 fs trukmės impulsai.

Šiame darbe buvo pademonstruotos skirtingos impulsų plėstuvo/spaustuvo konfigūracijos skaidulinėje čirpuotų impulsų stiprinimo sistemose. Ištirta skaidulinė čirpuotų impulsų stiprinimo sistema, kurioje impulsai plečiami skaiduline čirpuota Brego gardele, o spaudžiami difrakcinių gardelių pora. Skaitmeniniu modeliavimu buvo surastos sąlygos, kai difrakcinių gardelių spaustuvo įnešama trečios eilės dispersija riboja sistemos generuojamų impulsų laikinę kokybę. Skaitmeniniu modeliavimu ir eksperimentais buvo parodyta, jog tokioje sistemoje impulsų spaustuvo įnešamą trečios eilės dispersiją galima kompensuoti naudojant skaidulinę čirpuotą Brego gardelę su

optimaliu čirpo profiliu. Taip pat buvo ištirta skaidulinė čirpuotų impulsų stiprinimo sistema, kurioje impulsai plečiami valdomos dispersijos skaiduline čirpuota Brego gardele, o spaudžiami fiksuotos dispersijos čirpuota tūrine Brego gardele. Parodyta, kad tiesinio impulsų plėstuvo/spaustuvo čirpo profilio iškraipymas riboja tokios sistemos impulsų laikinę kokybę, kurią galima pagerinti tik naudojant suderintų dispersijos profilių dispersinius elementus.

Sukurtos ir šioje disertacijoje aprašytos skaidulinės čirpuotų impulsų stiprinimo sistemos, naudojančios pilnai skaidulinius užkrato šaltinius. Šiose sistemose 500 ps trukmės čirpuoti impulsai, kurių centrinis bangos ilgis buvo 1030 nm, didelio šerdies skersmens (40 µm ir 55 µm) fotoninių kristalų stiprintuvuose buvo sustiprinti iki 20-50 µJ energijos. Šių sistemų išėjime generuojami sub-300 fs trukmės impulsai.

Atlikti kontinuumo generacijos safyro, itrio aliuminio granato ir itrio vanadato kristaluose tyrimai žadinant 1 MHz pasikartojimo dažniu, 280 fs trukmės impulsais, generuojamais skaidulinio lazerio. Išmatuoti kontinuumo generacijos slenksčiai, generuojamo kontinuumo degradacija esant skirtingoms žadinančios spinduliuotės fokusavimo sąlygoms. Taip pat atlikti kontinuumo spinduliuotės stiprinimo BBO ir BiBO kristaluose eksperimentai. Nustatyta, jog BiBO kristale dėl didesnio kristalo netiesiškumo efektyvus kontinuumo spinduliuotės stiprinimas pasiekiamas prie 2,5 karto mažesnės kaupinimo impulsų energijos. Šie rezultatai leido realizuoti tokią lazerinę sistemą, kurioje generuojami 40-150 fs trukmės impulsai spektro ruože nuo 690 nm iki 2040 nm, kaupinant 1 µJ eilės energijos impulsais, generuojamais skaidulinio lazerio, veikiančio 1 MHz pasikartojimo dažniu. Šią spinduliuotės dažnio keitimo schemą bus siekiama komercializuoti kompanijoje EKSPLA, taip išplečiant gaminamų femtosekundinių skaidulinių lazerių taikymo sritis.

Curriculum Vitae

PERSONAL DETAILS

Name: **Saulius Frankinas**
Date of Birth: 1988.09.09
Place of Birth: Panevėžys
E-mail: s.frankinas@gmail.com

EDUCATION

2013–2017	Center for Physical Sciences and Technology, PhD studies, Physical sciences, Physics (02P).
2011–2013	Vilnius University, Master Degree, Laser physics and optical technologies.
2007–2011	Vilnius University, Bachelor Degree, Physics.
1995–2007	Panevezys Alfonsas Lipniunas Secondary School.

WORK EXPERIENCE

2012–now	EKSPLA Ltd., The Department of Research and Development– engineer.
2009–2011	Vilnius University, The Department of Quantum Electronics– engineer.